J Appl Electrochem (2007) 37:765–787
DOI 10.1007/s10800-007-9333-1

REVIEWS IN APPLIED ELECTROCHEMISTRY NUMBER 64

Hydrogen generation at irradiated oxide semiconductor–solution interfaces

Krishnan Rajeshwar

Received: 22 January 2007 / Accepted: 16 April 2007 / Published online: 22 May 2007

Abstract This review focuses on the use of inorganic oxide semiconductors for the photoassisted generation of hydrogen from water. Representative studies spanning approximately three decades are included in this review. The topics covered include a discussion of the types of water photosplitting approaches, an ideal photoelectrolysis system, an examination of why oxide semiconductors are attractive for this application, a review of both classical and more recent studies on titanium dioxide, tungsten trioxide, and other binary metal oxides, perovskites and other ternary oxides, tantalates and niobates, miscellaneous multinary oxides, semiconductor alloys and mixed semiconductor composites, and twin-photosystem configurations for water splitting.

Keywords Photoelectrolysis · Water splitting · Solar energy

1 Introduction and scope

This review article explores the possibility of using sunlight in conjunction with oxide semiconductor/solution interfaces for the production of hydrogen from water. The underlying principles of solar energy conversion using semiconductor/electrolyte interfaces have been discussed in several review articles, book chapters and books [1–22] and will not be repeated here. This field of ''photoelectrochemistry'' had its early origins in attempts to use inorganic semiconductor/electrolyte interfaces in electronic devices [23–28]. Subsequently, it was found in ca. 1970 that an electrochemical cell made from a n-TiO_2 photoanode and a Pt counterelectrode evolved H_2 and O_2 from water under UV irradiation or sunlight [29–33]. A flurry of activity ensued in the 1970s and 1980s on the photoelectrolysis of water; indeed, attempts to split water using sunlight and inorganic semiconductor(s) have continued in unabated manner to the present time.

K. Rajeshwar (✉)
Center for Renewable Energy Science & Technology (CREST), Department of Chemistry & Biochemistry, The University of Texas at Arlington, Arlington, TX 76019-0065, USA
e-mail: rajeshwar@uta.edu

2 Types of approaches

A bewildering array of terms have been deployed in this field; thus, a few clarifying remarks appear to be in order. The term ''photoelectrochemical'' refers to any scenario wherein light is used to augment an electrochemical process. This process could be either ''uphill'' (Gibbs free energy charge being positive) or ''downhill'' (negative ΔG) in a thermodynamic sense. In the former case, the process is called ''photosynthetic'' (the reaction $H_2O \rightarrow H_2 + 1/2\ O_2$ being an example) while the latter would be a photocatalytic process (e.g., the oxidation of hydrocarbons at an illuminated n-TiO_2/solution interface in an oxygenated medium). The term ''photoelectrolysis'' is correctly applied to a case involving semiconductor photoelectrode(s) in an electrochemical cell. The term ''photocatalysis'' has been generally applied to the case of semiconductor suspensions (see below). The term ''photoassisted splitting'' is recommended for cases wherein the excitation light energy only *partially* furnishes the voltage needed for the electrolysis process, the rest being accommodated by an applied external bias (see below). Finally, the term ''solar'' should be reserved for cases where sunlight (or at least simulated sunlight) was used for the semiconductor excitation. In all the cases, the more general term (or prefix) ''photo'' is appropriate.

Figure 1 illustrates the interfacial energetics involved in the photoelectrochemical evolution of H_2. Thus, the electronic energy levels in the semiconductor and in the contacting solution are shown on a common diagram. In a semiconductor, the filled electronic levels (valence band or VB) and the empty levels (conduction band or CB) are separated by a ''forbidden'' gap, namely, the band gap energy, E_g [34–36]. Photoexcitation of the semiconductor with light of energy equal to or exceeding E_g (i.e., with wavelengths corresponding to or shorter than that corresponding to the energy gap) elicits electron–hole pairs, a fraction of which (as defined by the quantum yield) escape recombination and find their way to the semiconductor/solution interface. For the photosplitting of water (Fig. 1a), the CB and VB edges at the semiconductor surface (E_{CB} and E_{VB} respectively) must bracket the two redox levels corresponding to the hydrogen evolution reaction (HER) and the oxygen evolution reaction (OER) respectively. This is tantamount to stating that the photogenerated electrons have sufficient energy to reduce protons and the photogenerated holes have sufficient energy to oxidize water (Fig. 1a).

This is a stringent requirement indeed as further elaborated in the next section. Instead of actually photosplitting water, sacrificial agents may be added to the solution such

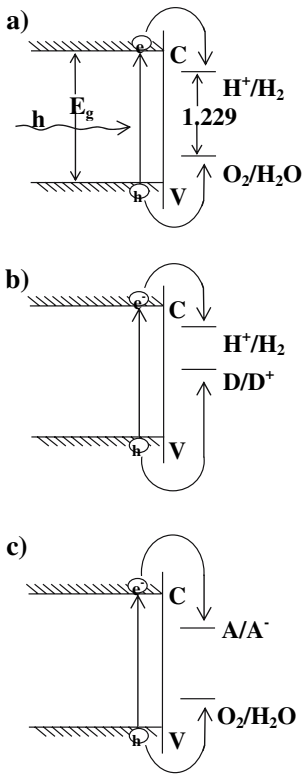

Fig. 1 Interfacial energetics at semiconductor–liquid junctions. D is an electron donor and A is an electron acceptor

that the HER and OER steps may be separately optimized and studied (Fig. 1b and c). It must be borne in mind that now the overall photoreaction becomes thermodynamically ''down-hill'' and is more appropriately termed: ''photocatalytic''(see above). Examples of sacrificial agents include sulfite for the photo-driven HER case (Fig. 1b) or Ag^+ as the electron acceptor for the photocatalytic oxidation of water (Fig. 1c).

Instead of using the semiconductor in the form of electrodes in an *electrochemical* cell, a ''wireless'' water splitting or HER system could be envisioned where particle suspensions are used (instead of electrodes) in a *photochemical* reactor. Two points regarding such an approach must be noted. First, unlike in the case of a semiconductor electrode, a bias potential cannot be applied in the suspension case. Second, the sites for the HER and OER are not physically separated as in the electrochemical case. Thus, the potential exists in a photochemical system for a highly explosive stoichiometric (2:1) mixture of H_2 and O_2 to be evolved. Nonetheless, strategies have been devised for immobilizing the semiconductor particles in a membrane so that the HER and OER sites are properly separated [37–43].

Bifunctional redox catalysts have been investigated in terms of their applicability for the solar-assisted splitting of water [1, 12, 44–52]. In this approach, Pt (an excellent catalyst for the HER) and RuO_2 (an excellent catalyst for the OER) are loaded onto colloidal TiO_2 particles. But unlike in the approaches discussed abover, the oxide semiconductor is not used as a light absorber; instead an inorganic complex [e.g., amphiphilic $Ru(bpy)_3^{2+}$ derivative, bpy = 2,2′-bipyridyl ligand] is used as the sensitizer [1, 12, 44]. Claims of cyclic and sustained water cleavage by visible light in this system, however, have not been independently verified. Since these ''microheterogeneous'' assemblies do not involve photoexcitation of a semiconductor, they are not further discussed here.

A photoelectrochemical (photoelectrolysis) system can be constructed using an n-type semiconductor electrode, a p-type semiconductor, or even mating n- and p-type semiconductor photoelectrodes as illustrated in Fig. 2a–c respectively. In the device in Fig. 2a, OER occurs on the semiconductor *photoanode* while the HER proceeds at a catalytic counterelectrode (e.g., Pt black). Indeed, the classical n-TiO_2 photocell alluded to earlier [29–33] belongs to this category. Alternately, the HER can be photodriven on a p-type semiconductor while the OER occurs on a ''dark'' *anode*.

Unlike the single ''photosystem'' cases in Fig. 2a and b, the approach in Fig. 2c combines two photosystems. Both heterotype (different semiconductors) or homotype (same semiconductor) approaches can be envisioned, and it has been shown [53] that the efficiency of photoelectrolysis

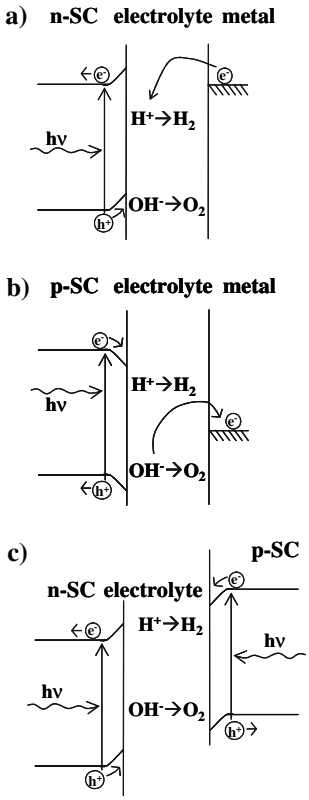

Fig. 2 Photoelectrolysis cell configurations (refer to text)

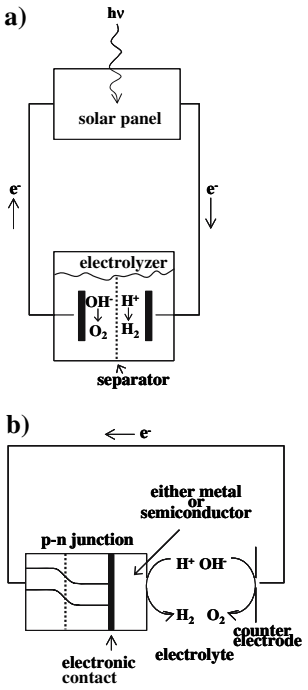

Fig. 3 Two hybrid photoelectrolysis cell configurations

with solar radiation can be enhanced by using simultaneously illuminated n- and p-type semiconductor electrodes (Fig. 2c). It is interesting to note that this twin-photosystems approach mimics the plant photosynthesis system, intricately constructed by nature, albeit operating at rather low efficiency. The approach in Fig. 2c has at least two built-in advantages. First, the sum of two photopotentials can be secured in an additive manner such that the required threshold for the water splitting reaction can be more easily attained than in the single photoelectrode cases in Fig. 2a and b. Second, different segments of the solar spectrum can be utilized in the heterotype approach, and indeed, many semiconductors (with different E_g's) can be stacked to enhance the overall solar conversion efficiency of the device [54, 55]. However, the attendant price to be paid is the concomitant increase in the device complexity. Further, the photocurrents through the two interfaces will have to be carefully matched since the overall current flowing in the cell must obviously be the same.

Finally, hybrid approaches for water photosplitting can be envisioned. As illustrated in Fig. 3a, a water electrolyzer can be simply hooked up to a solar panel that delivers the needed photovoltage [18, 55–57]. A conceptually more appealing scenario deploys a p–n junction directly in ohmic (electronic) contact with the electroactive surface where the HER (or less commonly, the OER) occurs (Fig. 3b). A variety of such ''monolithic'' configurations have been discussed, not all involving oxide semiconductors [58–62].For example, a p/n photochemical diode consisting of p-GaP and n-Fe_2O_3 has been assembled in a monolithic unit and studied for its capability to evolve H_2 and O_2 from seawater [63].

3 An ideal photoelectrolysis system

What photovoltage and semiconductor bandgap energy (E_g) would be minimally needed to split water in a single photosystem case (c.f., Fig. 2a or b)? To split water into H_2 and O_2 with both products at 1 atm, a thermodynamic potential of 1.23 V is needed. To this value would have to be added all the losses within an operating cell mainly related to resistive (Ohmic components) and the overpotentials (kinetic losses) required to drive the HER and OER at the two electrode/electrolyte interfaces. This would translate to a semiconductor E_g value of ~2 eV if the splitting of water to H_2 and O_2 is the process objective. On the other hand, photovoltaic theory [64] tells us that the photovoltage developed is nominally only ~60% of E_g. Taking all this into account, an E_g value around 2.5 eV would appear to be optimal.

What about a twin-photosystem configuration as in Fig. 2c? Optimal efficiency is reached in such a configuration when one semiconductor has an E_g value of ~1.0 eV and the second ~1.8 eV [65]. On the other hand, it has

been pointed out [66] that an optimal combination would be two matched electrodes of equal 0.9 eV band gap, since, in the absence of other limitations, the photocurrent would have been dictated by the higher E_g electrode of a pair.

An irradiated semiconductor particle in a microheterogeneous system can be regarded as a short-circuited electrochemical cell where that particle is poised at a potential (ΔV) such that the anodic and cathodic current components are precisely balanced (i.e., no *net* current obviously is flowing through that particle [67]. This photovoltage obviously has to attain a value around ~2 V for the water splitting reaction to be sustained. Given the need to reduce the kinetic losses and move the photovoltage value down to one around the thermodynamic (ideal) limit of 1.23 V, it is therefore not surprising that many of the studies on semiconductor particle suspensions have utilized (partially) metallized surfaces—the metals being selected to be catalytic toward the HER. The prototype here is the platinized semiconductor particle (e.g., Pt/TiO_2) and the platinum islands are deposited on the oxide surface using photolysis in a medium containing the Pt precursor (e.g., $PtCl_6^{2-}$) and a sacrificial electron donor (e.g., acetate) [68, 69]. Obviously, the bifunctional catalyst assemblies discussed earlier are motivated by considerations to make the HER and OER processes more facile. Very detailed studies also have appeared on catalytic modification of semiconductor *electrode* surfaces to improve the HER performance; the reader is referred to the many review articles and book chapters on this topic [1, 11, 70–73].

The earlier discussion related to Fig. 1a should have indicated that it is simply not the magnitude of E_g (and the ΔV generated) alone that is the sole criterion for sustaining the water photosplitting process. Where the CB and VB levels lie on the energy diagram for the semiconductor at the interface is crucial. Assuming that we are dealing with thermalized electrons here (i.e., no ''hot carrier'' processes), the CB edge for the n-type semiconductor has to be higher (i.e., be located at a more negative potential) relative to the H_2/H^+ redox level in the solution (c.f., Fig. 1a). In the event that this is not true (see Fig. 4), an external bias potential would be needed to offset the deficit energy content of the photogenerated electrons. Other equivalent statements can be made for the requirements for an n-type semiconductor, namely that the semiconductor has to have low electron affinity or that the flat-band potential for that particular semiconductor/electrolyte interface has to be more negative than the H_2/H^+ redox level.

Interestingly, rutile TiO_2 electrodes have an interfacial situation similar to that schematized in Fig. 4. Thus, the authors in the classical n-TiO_2 water splitting study [29–33] circumvented this problem via a *chemical* bias in their electrochemical cell by imposing a pH gradient between the photoanode and cathode chambers. On the other hand,

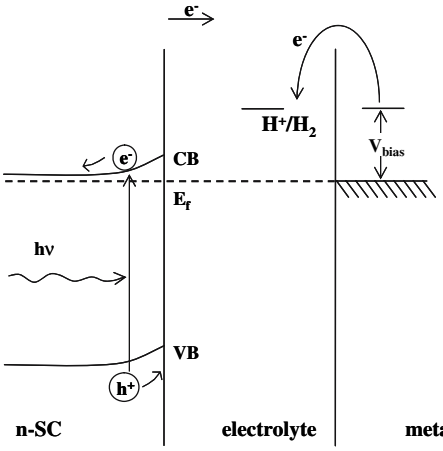

Fig. 4 An interfacial energetic situation in a photoelectrolysis cell where the flat-band potential of the n-type semiconductor photoanode lies positive of the HER potential. V_{bias} is the external bias potential needed in this case to drive the photoelectrolysis process

photogenerated holes in TiO_2 are generated at a very positive potential (because of its low-lying VB edge at the interface) so that they have more than enough energy to oxidize water to O_2. Not too many semiconductor surfaces are stable against photocorrosion under these conditions; i.e., the photogenerated holes attack the semiconductor itself rather than a solution species such as OH^- ions. The requirements for a single photosystem for splitting water should have semiconductor energy levels that straddle the two redox levels (H_2/H^+ and OH^-/O_2), have an E_g value of ~2.5 eV for the semiconductor, and with a semiconductor surface that is completely immune to photocorrosion under OER (or HER) conditions. Additionally, the semiconductor surface has to be made catalytically active toward OER or HER.

Interfacial energetics in two-photosystem cells combining n- and p-type semiconductor electrodes respectively (Fig. 2c) have been discussed [74]. Stability issues in photoelectrochemical energy conversion systems have been reviewed [9, 13, 14].

In a regenerative solar energy conversion system, the device efficiency (η) is simply given by the ratio of the power delivered by the photovoltaic converter and the incident solar power (P_s in W m^{-2} or mW cm^{-2}). However, we are concerned here with devices producing a fuel (H_2) and several expressions exist for the device efficiency. Thus, this efficiency can be expressed in kinetic terms [55, 75]:

$$\eta_1 = \frac{\Delta G^{o}_{H_2} R_{H_2}}{P_s A} \times 100 \qquad (1)$$

In Eq. 1, ΔG^{o}_{H2} is the standard Gibbs energy for the water splitting reaction generating H_2,R_{H2} is the rate (mol s^{-1}) of

generation of H_2, and A is the irradiated area (m^2 or cm^2). In the above (as well as in the expression below), it is assumed that the H_2 gas is evolved at 1 atm in its standard state. (Corrections have been discussed for cases where the gas is not evolved at 1 atm, see [55]) Another equation for the efficiency refers to the standard (Nernstian) voltage for the water splitting reaction, 1.23 V [13]:

$$\eta_2 = \frac{(1.23 - V_{\text{bias}})\, i_t}{P_s A} \times 100 \qquad (2)$$

The bias voltage, that is needed in some cases is V_{bias} and i_t is the current corresponding to the maximum power point [11, 65] of the cell.

In some cases, ΔH values are used in place of the free energy, and then the term, 1.23 in Eq. 2, must be replaced with 1.47. This assumes that the products will be burned (i.e., in a thermal combustion process) to recover the stored energy as heat rather than as electrical energy in a fuel cell. Other efficiency expressions have been proposed that take into account the energy throughput or the polarization losses at the photoelectrode(s) and the ''dark'' counter-electrode where relevant (see for example, [76]). The shortcomings of these alternate expressions have been pointed out [13]. In cases where the energy storage system generates a multitude of products rather than just H_2, the free energy term in the numerator in Eq. 1 becomes a summation of all the free energies stored in the various products [77].

What about ideal and achievable efficiency values in photoelectrolytic cells? Discussions exist for ideal limits of process efficiency values [13, 55, 75, 78, 80]. Taken as a whole, a 10–12% process efficiency (under, say, AM 1.0 solar irradiation) for a solar photoelectrochemical water splitting system based on a *single* photoconverter, appears to be a reasonable target. Higher efficiencies can be realized in a multi-photosystem or even a tandem (i.e., hybrid, see above) configuration although attendant increase in costs associated with increased system complexity may have to be taken into account here. The sensitivity of η to parameters such as the semiconductor band gap (E_g) has been analyzed by several authors [78–80]. The efficiency peaks at ~1.5 eV and ~2.2 eV for a twin- and a one-photosystem respectively [79, 80] and at ~1.8 eV for a tandem cell combining a solar photovoltaic cell with a single photoanode-based electrochemical cell [55].

The search for satisfactory semiconductor candidates has continued at an unabated rate to the time of writing of this article. In a historical sense, it is interesting that the shift of the research objective from initially photoelectrolysis toward regenerative photoelectrochemical cells (which generate electricity rather than a fuel such as H_2) in the early years (1980s) is undoubtedly a consequence of the many challenges involved in the discovery (and optimization) of a semiconductor for the solar water splitting application.

3.1 Why oxide semiconductors

Oxide semiconductors are eminently attractive candidates as the photocatalyst materials for photoelectrochemical H_2 generation. A sizable fraction of the total cost of the solar photoelectrolysis assembly resides with the semiconductor photocatalyst itself. Thus given that silicon itself is not an optimal semiconductor for photoelectrochemical H_2 generation, because of stability problems and an insufficient E_g value of 1.1 eV (see above), the remaining option would be compound semiconductors drawn from Groups II, III, V, and VI in the Periodic Table. However, semiconductors containing elements such as Ga or In are hardly attractive because of the scarcity of these metals while compounds such as GaAs, CdTe and CdSe would suffer from concerns with elemental toxicity and concomitant environmental issues associated with materials disposal after the device lifetime. This then leaves oxide semiconductors as the photocatalyst materials of choice for the H_2 generation application.

Oxide semiconductors are generally prepared by ceramic (high-temperature) routes. This would be a handicap for *energy* applications of the synthesized materials. The net energy gain (NEG) is an important concept in energy economics and this refers to the surplus between the energy required to harvest an energy source (in this case, the semiconductor) and the energy provided by that same source. The lower the external energy input for the semiconductor synthesis, the lower the energy payback time (or the higher the NEG). This is where low-temperature synthesis routes such as electrodeposition [81], chemical bath deposition [82], or energy-efficient approaches to semiconductor synthesis such as combustion synthesis [83], become strategically very important.

4 Photoelectrochemistry of oxide semiconductors—early work

The use of oxide semiconductors for the photoelectrolysis of water has been reviewed [84, 85]. Eleven binary and ternary oxides were examined in the first review [84]. Linear correlations were presented between the flat band potential, V_{fb} of these oxides and their band gap energy (E_g); and between V_{fb} and the heat of formation of the oxide per metal atom per metal-oxygen bond. Aligning all the oxide energy levels on a common scale, these authors noted [84] that the position of the conduction band varies

much more than those of valence bands—a trend expected from the cationic (d-band) character of the conduction band in the oxide while the valence band is mainly of O(2p) character. The latter should be relatively independent of the oxide parentage in terms of the metal.

A similar correlation between V_{fb} and E_g was presented [85] but for a much more extensive collection of oxides including oxides with or without partially filled d levels and oxides formed anodically on metals. Only oxides with partially filled d levels (Type ''a'' in the author's notation [85]) yielded a straight-line correlation between the two parameters. This plot was used by the authors of the two studies [84, 85] for predictive purposes to assess the efficacy of a given oxide for the photoelectrolysis of water. As seen earlier, the V_{fb} of the material has to be at a negative enough potential to drive the HER, and E_g has to be ~2 eV and yet bracket the HER and OER redox levels (c.f., Fig. 1a).

The possibility of introducing new d-bands for Type ''b'' oxides (with filled d-bands) by introducing dopants into the host lattice was also discussed [85] with examples. Other authors have also advocated this approach [86]. A review [14] contains further examples of this approach for effectively ''shrinking'' the original E_g and sensitizing the oxide to visible portions of the solar spectrum. We shall return to this aspect for the specific case of TiO_2 later in this chapter.

We now turn to discussions of individual oxide semiconductor materials for the photoelectrolysis of water, starting with the ''mother'' of all oxides, namely, TiO_2.

5 Titanium dioxide early work

Historically, this is the material which really sparked interest in the solar photoelectrolysis of water. Early papers on TiO_2 mainly stemmed from the applicability of TiO_2 in the paint/pigment industry [87] although fundamental aspects such as current rectification in the dark (in the reverse bias regime) shown by anodically formed valve metal oxide film/electrolyte interfaces was also of interest (e.g., [28]). Another driver was possible applications of UV-irradiated semiconductor/electrolyte interfaces for environmental remediation [67, 88, 89].

Representative early work on this remarkable material is presented in chronological order in Table 1, with all these studies aimed toward the photoelectrolysis of water. Further summaries of this early body of work are available [2, 4, 9, 14].

5.1 Studies on the mechanistic aspects of processes at the TiO_2-solution interface

Also contained in the compilation in Table 1 are some early studies oriented toward the *mechanistic* aspects of the photoelectrochemical oxidation of water (and other compounds) at the n-TiO_2-electrolyte interface, as exemplified by Entries 23 and 29 [109, 115]. There are recent and representative studies of this genre [121–153].

5.2 Visible light sensitization of TiO_2

Rather problematic with TiO_2 in terms of the attainable process efficiency is its rather wide band gap (3.0–3.2 eV). Consequently, only a small fraction (~5%) of the overall solar spectrum can be harnessed by this material. Thus, the early work (as in Table 1, Entries 16 and 17 [102, 103] respectively) has also included attempts at extending the light response of TiO_2 from the UV to the visible range [for example, 123, 154–160]. Reviews of these works are available [14, 161–163]. For reasons mentioned earlier, we exclude for our discussion, studies oriented toward chemical modification of the TiO_2 surface with a dye. As summarized elsewhere [162, 163]transition metal dopants also modify the interfacial charge transfer and electron–hole recombination behavior of the TiO_2 host. Whether a given dopant exerts a positive or negative effect depends on the particular metal [162, 163].

It must be noted that most studies on metal-doped TiO_2 are oriented toward the photo-oxidation of environmental pollutants (e.g., 4-nitrophenol [164] 4-chlorophenol [165]) rather than toward the photoelectrolysis of water. Other aspects of metal doping include the effect of UV radiation of Ag-doped TiO_2 specimens [166, 167] and plasma treatment [168]. Metal doping by ion implantation of TiO_2 has been discussed [169, 170]. Noble-metal doped (not chemically modified, see above) TiO_2 samples are also of interest [171].

Non-metallic elements such as fluorine, carbon, nitrogen and sulfur have been incorporated into TiO_2. Table 2 contains a compilation of representative studies on this topic. As with the trend noted earlier with metal dopants, very few of the studies in Table 2 are oriented toward water photosplitting or OER [175, 185, 187]. Other than the desired optical response, non-metallic dopants also exert electronic effects on the host behavior as with the metal dopants (see above). Thus F-doping is observed to cause a reduction in the e^-–h^+ recombination rate [188]while N-doping at high levels has the opposite effect and serves to suppress the photocatalytic activity of the TiO_2 host [181]. Conflicting views exist on non-metal doping, particularly with respect to the mechanistic aspects [181].

5.3 Recent work on TiO_2 on photosplitting of water or on the oxygen evolution reaction

Table 3 contains a compilation of studies that have appeared since 1985. Several points are worthy of note

Table 1 Representative examples of work prior to ~1985 on the use of TiO_2 for the photoelectrolysis of water

Entry number	Title of article	Comments	Reference(s)
1	Electrochemical Photolysis of Water at a Semiconductor Electrode	First demonstration of the feasibility of water splitting.	[30]
2	The Quantum Yield of Photolysis of Water on TiO_2 Electrodes	Very low quantum yields (~10^{-3}) were measured when no external bias was applied. The effect of photon flux also explored.	[90]
3	Photoelectrolysis of Water Using Semiconducting TiO_2 Crystals	Study shows the necessity of a bias potential for rutile photoanodes.	[91]
4	Photoelectrolysis of Water in Cells with TiO_2 Anodes	Both single crystal and polycrystalline TiO_2 used and external quantum efficiency measured.	[92]
5	A Photo-Electrochemical Cell with Production of Hydrogen and Oxygen by a Cell Reaction	Cell configuration also employs an illuminated p-GaP photocathode (c.f. Ref. 53).	[93]
6	Photoassisted Electrolysis of Water by Irradiation of a Titanium Dioxide Electrode	The initial claim in Ref. 30 supported along with data on the wavelength response and the correlation of product yield and current.	[94]
7	Semiconductor Electrodes 1. The Chemical Vapor Deposition and Application of Polycrystalline n-Type Titanium Dioxide Electrodes to the Photosensitized Electrolysis of Water	Comparison of the behavior of CVD and single crystal n-TiO_2 presented.	[95]
8	Formation of Hydrogen Gas with an Electrochemical Photo-cell	See text.	[31]
9	Hydrogen Production under Sunlight with an Electrochemical Photo-cell	See text.	[32]
10	Photoproduction of Hydrogen: Potential Dependence of the Quantum Efficiency as a Function of Wavelength	–	[96]
11	Photoelectrolysis of Water with TiO_2-Covered Solar-Cell Electrodes	A hybrid structure, involving a p-n junction Si cell coated with a TiO_2 film by CVD, is studied.	[97]
12	Electrochemical Investigation of an Illuminated TiO_2 Electrode	Two types of TiO_2 films studied, namely, anodically formed layers on Ti sheets and those prepared by plasma jet spraying of TiO_2 powder.	[98]
13	Intensity Effects in the Electrochemical Photolysis of Water at the TiO_2 Anode	Quantum efficiency observed to approach unity at low light intensities.	[99]
14	Improved Solar Energy Conversion Efficiencies for the Photocatalytic Production of Hydrogen via TiO_2 Semiconductor Electrodes	Heat treatment of Ti metal found to influence performance.	[100]
15	Near-UV Photon Efficiency in a TiO_2 Electrode: Application to Hydrogen Production from Solar Energy	–	[101]
16	Novel Semiconducting Electrodes for the Photosensitized Electrolysis of Water	Appears to be the first study on doping TiO_2 to extend its light response into the visible range of the electromagnetic spectrum.	[102]
17	Photoelectrolysis of Water in Sunlight with Sensitized Semiconductor Electrodes	Similar observations as in Ref. 102 for Al^{3+}-doped TiO_2.	[103]
18	Photoelectrolysis	The behavior of single crystals of two different orientations (⊥ and ∥ to the C axis) and polycrystalline TiO_2 reported.	[104]
19	The Quantum Yields of Photoelectric Decomposition of Water at TiO_2 Anodes and p-Type GaP Cathodes	A more detailed study as in Ref. 103 by the same research group.	[105]
20	Anomalous Photoresponse of n-TiO_2 Electrode in a Photo-electrochemical Cell	The behavior of surface states at the TiO_2-electrolyte interface is focus of this study.	[106]
21	An Effect of Heat Treatment on the Activity of Titanium Dioxide Film Electrodes for Photosensitized Oxidation of Water	Heat treatment in argon atmosphere found to improve performance of both anodic and pyrolytically prepared TiO_2 films.	[107]
22	Preparation of Titanium Dioxide Films as Solar Photocatalysts	Low-cost polyimide plastic used as film substrate.	[108]

Table 1 continued

Entry number	Title of article	Comments	Reference(s)
23	Photoelectrochemical Behavior of TiO_2 and Formation of Hydrogen Peroxide	Other than the OER, reduction of O_2 to H_2O_2 also observed.	[109]
24	Photodeposition of Water over Pt/TiO_2 Catalysts	Powdered photocatalyst is employed.	[110]
25	Photocatalytic Decomposition of Gaseous Water over TiO_2 and TiO_2–RuO_2 Surfaces	As above but gaseous water used at room temperature.	[111]
26	Photoelectrolysis of Water with Natural Mineral TiO_2 Rutile Electrodes	Natural samples compared with Fe-doped synthetic single crystal TiO_2.	[112]
27	Models for the Photoelectrolytic Decomposition of Water at Semiconducting Oxide Anodes	Although title is general, theoretical study focuses on the TiO_2-electrolyte interface and the effect of surface states.	[113]
28	Photosynthetic Production of H_2 and H_2O_2 on Semiconducting Oxide Grains in Aqueous Solutions	Hydrogen peroxide formation observed in TiO_2 powder *suspensions* as in Ref. 109 for TiO_2 *films*.	[114]
29	Influence of pH on the Potential Dependence of the Efficiency of Water Photo-oxidation at n-TiO_2 Electrodes	Quantum efficiency for water photooxidation is shown to be pH-dependent.	[115]
30	Photocatalytic Water Decomposition and Water-Gas Shift Reactions over NaOH-Coated, Platinized TiO_2	As in Entry 24 (Ref. 110) by the same research group.	[116]
31	Photosensitized Dissociation of Water using Dispersed Suspensions of n-Type Semiconductors	Focus of study on TiO_2 and $SrTiO_3$ using EDTA as an electron donor and Fe^{3+} as acceptor for tests of water reduction and oxidation activity respectively (c.f. Figures 1b and 1c).	[117]
32	Photocatalytic Hydrogen Evolution from an Aqueous Hydrazine Solution	Pt-TiO_2 photocatalyst used and both H_2 and N_2 evolution observed.	[118]
33	Conditions for Photochemical Water Cleavage. Aqueous Pt/TiO_2 (Anatase) Dispersions under Ultraviolet Light	As in Entries 24 and 25 (Refs.110,111) photocatalyst dispersions studied.	[119]
34	Colloidal Semiconductors in Systems for the Sacrificial Photolysis of Water. 1. Preparation of a Pt/TiO_2 Catalyst by Heterocoagulation and its Physical Characterization	–	[120]

here. The vast majority of the entries feature studies on TiO_2 powders rather than on electrodes in a photoelectrochemical cell configuration. In this light, the new studies can be regarded as offshoots inspired by the earlier (pre-1985) studies on co-functional photocatalysts and the cyclic cleavage of water [1, 12]. Second, many of the new studies address two key issues with the earlier systems: (a) non-stoichiometric evolution of H_2 and O_2 and (b) poor performance stemming from back reactions and electron–hole recombination processes. With reference to the first point, very little O_2 evolution was observed in many cases in studies on TiO_2 powder suspensions with reports [111, 191, 195] of stoichiometric H_2 and O_2 evolution (i.e., in the expected 2:1 ratio) being the exceptions rather than the rule. Initially, this discrepancy was attributed by the community to the photo-induced adsorption of the (evolved) O_2 on the TiO_2 surface.

The remarkable effect of a NaOH ''dessicant'' coating on the TiO_2 surface on the efficiency of water photosplitting appears to have radically changed this thinking (see [211] and references therein). The new results support the deleterious role that Pt islands on the TiO_2 play in promoting the reverse reaction, $2H_2 + O_2 \rightarrow 2H_2O$. Interestingly, the irradiation geometry also appears to exert an effect on the extent of back reactions [212]. Adsorption of CO on Pt, for example, was also found to inhibit the reverse reaction [213]. Subsequent studies on the role of Na_2CO_3 addition ([214] and Entries 3 and 4 in Table 3) underline the importance of inhibiting back reactions on catalyst-modified TiO_2 samples. By the same token, unusual valence states (Ti^{5+}) that have been proposed [199] to explain the non-stoichiometric gas evolution have been challenged by other authors [215].

Other factors influencing the yield of H_2 and O_2 in irradiated TiO_2 suspensions include the nature of the co-catalyst (see, for example, Entry 4 in Table 3), the crystal form of TiO_2, particle size of TiO_2, temperature and ambient pressure [211]. The reader is referred to [211] for further details. Other interesting mechanistic aspects of the water photosplitting process on the TiO_2 surface such as hydrogen atom spillover have also been discussed [216].

Table 2 Representative studies on doping of TiO_2 with non-metallic elements

Entry number	Title of article	Comments	Reference(s)
1	Visible-Light Photocatalysis in Nitrogen-Doped Titanium Oxides	Both films and powders considered. Substitutional doping with nitrogen shown to bring about band gap narrowing and also high photocatalytic activity with visible light. Experimental data supported with first-principles calculations.	[172]
2	Formation of $TiO_{2-x}F_x$ Compounds in Fluorine-Implanted TiO_2	Fluorine substituted for oxygen sites in the oxide by ion implantation.	[173]
3	Band Gap Narrowing of Titanium Dioxide by Sulfur Doping	Oxidative annealing of TiS_2 used. Ab initio calculations also reveal mixing of S 3p states with the valence bond to bring about band gap narrowing.	[174]
4	Efficient Photochemical Water Splitting by a Chemically Modified n-TiO_2	Combustion of Ti metal in a natural gas flame done to substitute carbon for some of the lattice oxygen sites. The photocatalysis performance data have been questioned (see Refs. 176–178).	[175]
5	Daylight Photocatalysis by Carbon-Modified Titanium Dioxide	Titanium tetrachloride precursor hydrolyzed with nitrogen bases to yield (surprisingly) C-doped (instead of N-doped) TiO_2. Study oriented toward environmental remediation applicability.	[179]
6	Carbon-Doped Anatase TiO_2 Powders as a Visible-Light Sensitive Photocatalyst	Oxidative annealing of TiC used to afford yellow doped powders. Study focus as in Entry 5.	[180]
7	Nitrogen-Concentration Dependence on Photocatalytic Activity of $Ti_{2-x}N_x$ Powders	Samples prepared by annealing anatase TiO_2 under NH_3 flow at 550–600 °C.	[181]
8	Visible Light-Induced Degradation of Methylene Blue on S-doped TiO_2	As in Entry 3 (Ref. 174) by the same research group.	[182]
9	Visible-Light Induced Hydrophilicity on Nitrogen-Substituted Titanium Dioxide Films	Degree of hydrophilicity correlated with the extent of substitution of nitrogen at oxygen sites.	[183]
10	Spectral Photoresponses of Carbon-Doped TiO_2 Film Electrodes	Raman spectra used to identify disordered carbon in the flame-formed samples in addition to lower nonstoichiometric titanium oxides identified by X-ray diffraction.	[184]
11	Photoelectrochemical Study of Nitrogen-Doped Titanium Dioxide for Water Oxidation	One of the few studies probing the influence of doping on OER.	[185]
12	Metal Ion and N Co-doped TiO_2 as a Visible-Light Photocatalyst	Co-doped samples prepared by polymerized complex or sol-gel method. Doped N species found to reside at interstitial lattice positions in the host.	[186]
13	Novel Carbon-Doped TiO_2 Nanotube Arrays with High Aspect Ratios for Efficicient Solar Water Splitting	–	[187]

An interesting aspect of the new work on TiO_2, namely that of combining two photosystems (in a Z-scheme) mimicking plant photosynthesis (see Entries 6 and 10 in Table 3) also has its roots in early work in this field (see, for example, Entry 5 in Table 1). Further elaborations of this strategy are available [217, 218].

Finally, some of the studies considered in Table 3 (Entries 11 and 13) buck the trend mentioned earlier that few of the studies on transition-metal doped TiO_2 are oriented toward the water-photosplitting application. These new studies exploit the visible-light sensitization of the doped host material as well as the improved electronic characteristics observed in some cases (particularly the co-doped instance) to enhance the efficiency of the water photosplitting process.

In sum, TiO_2 continues to be a veritable workhorse of the photocatalysis and photoelectrolysis communities. Studies of the electrical properties and defect chemistry continue to appear for this material in both single crystal [219–222] and nanostructured form [223]. Yet this material to date has not yielded systems for evolving H_2 and O_2 at the 10% benchmark efficiency level. Studies on TiO_2 oriented toward visible light sensitization and efficiency enhancement will undoubtedly continue, at an unabated rate, in the foreseeable future. This is because of the extensive and growing market that already exists for this commodity chemical in a variety of *other* application areas and because of its excellent chemical attributes such as inertness and stability.

6 Other binary oxides

Table 4 contains a compilation of studies on other binary oxides that have been examined for their applicability to

Table 3 Representative studies since 1985 on the photosplitting of water using TiO_2

Entry Number	Brief outline of study	Reference(s)
1	Ferroelectric substrates (poled $LiNbO_3$) were used to support TiO_2 films. After platinization of TiO_2, water splitting was examined in both liquid and gas phases under Xe arc lamp illumination.	[189]
2	Both reduced and Pt-modified powder samples were studied in distilled water and in aqueous solutions of HCl, H_2SO_4, HNO_3 and NaOH. Water photodecomposition proceeds moderately in distilled water and in NaOH but is strongly suppressed in acidic aqueous media. The NaOH coating effect mimicks that found by other workers earlier (see Ref. 191 and text).	[190]
3	Sodium carbonate addition to a Pt/TiO_2 suspension in water effective in promoting stoichiometric photodecomposition of water.	[192, 193]
4	Demonstration of solar H_2 and O_2 production on NiO_x/TiO_2 co-catalyst with Na_2CO_3 or NaOH addition.	[194, 195]
5	A photoelectrolyzer designed with a TiO_2 photoanode and a membrane of sulfonated polytetrafluoroethylene as the electrolyte. A quantum efficiency of 0.8 was reported.	[196]
6	Photochemical splitting of water achieved by combining two photocatalytic reactions on suspended TiO_2 particles; namely, the reduction of water to H_2 using bromide ions and the oxidation of water using Fe(III) species. High efficiency also observed for the photoassisted OER on TiO_2 in the presence of Fe(III) ions.	[197, 198]
7	Pt- and other catalyst supported TiO_2 (P-25) particles studied. Only the HER was observed and stoichiometry H_2 and O_2 formation was not found. Mechanistic reasons proposed have been challenged by other authors (see text).	[199]
8	HER observed in semiconductor septum cells using TiO_2 or TiO_2–In_2O_3 composites.	[41, 42]
9	Pure rutile TiO_2 phase isolated from commercial samples containing both rutile and anatase by dissolution in HF. The resultant samples studied for their efficacy in driving the photoassisted OER in the presence of Fe(III) species as electron acceptor (see Entry 6 above).	[200]
10	A Z-scheme system mimicking the plant photosynthesis model developed with Pt-loaded TiO_2 for HER and rutile TiO_2 for OER. An IO_3^-/I^- shuttle was used as redox mediator.	[201]
11	Co-doping of TiO_2 with Sb and Cr found to evolve O_2 from an aqueous $AgNO_3$ solution under visible light irradiation.	[202]
12	HER observed from a mixed water-acetonitrile medium containing iodide electron donor and dye-sensitized Pt/TiO_2 photocatalysts under visible light irradiation.	[203]
13	Back-reactions (i.e., O_2 reduction and H_2 oxidation) studied on both TiO_2 or Cr and Sb co-doped TiO_2 samples (see Entry 11 above).	[204]
14	TiO_2 nanotube arrays prepared by anodization of Ti foil in a F^--containing electrolyte. Pd-modified photocatalyst samples show an efficiency of 4.8% based on photocurrent data for the OER.	[205–209]
15	TiO_2 co-doped with Ni and Ta (or Nb) show visible light activity for the OER in aq. $AgNO_3$ and HER in aqueous methanol solution.	[210]

drive the photoelectrolysis of water. As cited earlier, general reviews are available on many of the oxides listed in this table [4, 14, 84, 85]. Other than TiO_2, Fe_2O_3 and WO_3 are two of the most widely studied among the binary oxide semiconductors, and studies on these oxides have continued to appear right up to the time of the writing of this chapter.

Tungsten oxide shares many of the same attributes with TiO_2 in terms of chemical inertness and exceptional photoelectrochemical and chemical stability in aqueous media over a very wide pH range. However, its flat-band potential (V_{fb}) lies positive of that of TiO_2 (anatase) such that spontaneous generation of H_2 by the photogenerated electrons in WO_3 is not possible. This location of V_{fb} has been invoked [232] for the very high IPCE values observed for the photoinduced OER in terms of the rather slow back electron transfer leading to O_2 reduction. A variety of dopants (e.g., F, Mg, Cu) have been tested for WO_3[226, 229, 235] and Pt-modified samples have been deployed in a Z-scheme configuration [234]. Electron acceptors such as Ag^+ [228] and IO_3^-[234] species have been used to study the O_2 evolution characteristics of the WO_3 photocatalyst under visible light irradiation. As pointed out very early in the history of study of this material [218, 269] the lower E_g value of WO_3 (relative to TiO_2) results in a more substantial utilization of the solar spectrum. This combined with the advances in nanostructured oxide materials will likely sustain interest in WO_3 from a photoelectrolysis perspective.

Table 4 Binary oxides (other than TiO_2) that have been considered for the photoelectrolysis of water

Entry number	Oxide semiconductor	Energy band gap, eV	Comments	Reference(s)
1	WO_3	2.5–2.8	This material has been used as single crystals, thin films, powders and in mesoporous/nanostructured form. Both virgin and doped samples studied.	[224–235]
2	Fe_2O_3	2.0–2.2	As in Entry 1 above.	[236–255]
3	ZnO	3.37	Unstable under irradiation and OER/HER conditions.	[114]
4	SnO_2	3.5	Sb-doped single crystal samples used. Stable H_2 and O_2 evolution observed at Pt cathode and SnO_2 photoanode respectively.	[256, 257]
5	NiO	3.47	A p-type semiconductor with indirect gap optical transition.	[258–260]
6	CdO	~2.3	A n-type semiconductor. Interestingly, RuO_2-modified samples reduced the yield of O_2 under irradiation.	[261]
7	PdO	~0.8	A p-type semiconductor. Not stable under irradiation in the HER regime.	[262]
8	Cu_2O	2.0–2.2	Claims of water splitting in powder suspensions challenged by others (see text).	[263, 264]
9	CuO	1.7	Not photoelectrochemically stable.	[239, 265]
10	Bi_2O_3	2.8	Both doped and catalytically modified samples studied.	[239, 266–268]

The combination of a rather low E_g value, good photoelectrochemical stability and chemical inertness coupled with the abundance of iron on our planet makes Fe_2O_3 an attractive candidate for the photoelectrolysis of water. Thus it is hardly surprising that this material continues to be intensively studied from this perspective. As with TiO_2 and WO_3, Fe_2O_3 (particularly the α-modification) has been examined in single crystal form, as thin films prepared by CVD [237, 239, 255, 270], pyrolytic conversion of iron [240], and spray pyrolysis [248, 250–253], or as sintered pellets from powders [241–246]. A variety of dopants have been deployed to modify the host [242–245, 247, 250–253] and remarkably, p-type semiconductor behavior has been reported [242, 244, 245, 251] in addition to the more commonly occurring n-type material. The main handicap with Fe_2O_3 is its rather poor electronic and charge transport characteristics regardless of the method of preparation of the material. Specifically, facile e^-–h^+ recombination, trapping of electrons at defect sites and the poor mobility of holes conspire to result in very low efficiencies for water oxidation. Attempts to circumvent these problems by using unique photoanode configurations (e.g., nanorod arrays [249]) or compositional tuning (e.g., minimizing sub-stoichiometric phases such as Fe_3O_4 [246, 253]) are continuing and will undoubtedly contribute to further examinations of this promising material in the future.

By way of contrast, none of the other binary oxides listed in Table 4 appear to hold much promise. While ZnO has enjoyed extensive popularity in the photochemistry community (even comparable to TiO_2 in the early days prior to ~1980), it is rather unstable (at least in the forms synthesized up till now) under illumination and in the OER and HER regimes. This problem besets most of the other candidates in Table 4 with the exception of SnO_2 (whose E_g is too high) and possibly Bi_2O_3. The report [263] of photocatalytic water splitting on Cu_2O powder suspensions (with stability in excess of ~1900 h!) has been greeted with scepticism by others [264] who have also pointed out that the Cu_2O band-edges are unlikely to bracket the H^+/H_2 and O_2/H_2O redox levels as required (see Fig. 1a). Our own studies [271] on electrodeposited samples of this oxide have utilized a Ni/NiO protective layer, catalyst modification (with e.g., Pt) to drive the HER and the use of optimized electron donors in the anode compartment in a twin-compartment photoelectrochemical cell (Fig. 5)

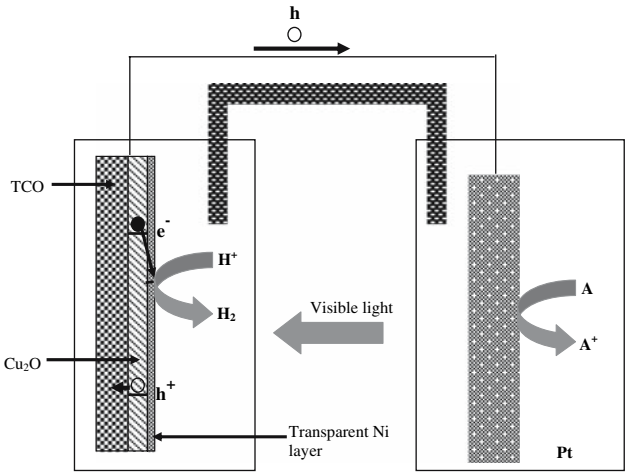

Fig. 5 Twin-compartment photoelectrochemical cell for the photocatalytic generation of H_2 from water using electrodeposited p-Cu_2O (from Ref. 253). TCO is a transparent conducting oxide substrate for the semiconductor film and A is an electron donor in the anode compartment

[271]. Under these conditions, spontaneous HER was observed under visible light irradiation of the p-Cu_2O photocathode. Photoinduced transfer of electrons from p-Cu_2O to an electron acceptor such as methyl viologen was also demonstrated via in situ spectroscopic monitoring of the blue cation radicals [271]. However, the photocurrents generated are only in the μA level necessitating further improvements before assessments of practical viability of Cu_2O for solar H_2 photogeneration. A value added approach would be to combine photogenerated H_2 generation with destruction of an environmental pollutant (e.g., dye) in the other compartment of a divided electrochemical cell [271–273].

It is worth noting that some oxides have *too low* a band gap for optimal solar energy conversion. Palladium oxide in Table 4 exemplifies this trend as does PbO_2 [239] On the other hand, PbO has an E_g value around 2.8 eV [239]. Other oxides such as CoO and Cr_2O_3 (both p-type semiconductors) have been very briefly examined early on in the evolution of this field [239].

In closing this section, comparative studies on binary oxide semiconductors are available [84, 85, 239, 274] including one study [274] where the electron affinities of several metal oxides (used as anodes in photoelectrolysis cells) were calculated from the atomic electronegativity values of the constituent elements. These electron affinity estimates were correlated with the V_{fb} values measured for the same oxides in aqueous media [274].

7 Perovskite titanates and related oxides

Perovskites have the general formula, ABX_3, with $SrTiO_3$ being a prototype. They contain a framework structure containing corner-sharing TiO_6 octahedra with the A cation in twelve-coordinate interstices [275, 276]. Several hundred oxides have this structure. Table 5 lists the studies that have appeared on $SrTiO_3$ with photoelectrolysis of water as a primary objective. As well as the cubic structure exemplified by $SrTiO_3$, a variety of distorted, non-cubic structures occurs in which the framework of TiO_6 octahedra may be twisted. Thus, $BaTiO_3$ is tetragonal at room temperature. Both $SrTiO_3$ and $BaTiO_3$ have energy band gaps around 3.2 eV. With Fe and F doping, the E_g of $BaTiO_3$ has been shrunk from 3.2 eV to ~2.8 eV [304]. Relative to $SrTiO_3$, studies on $BaTiO_3$ from a photoelectrolysis perspective are much sparser [304–306].

Titanates with tunnel structures have been examined for photoelectrolysis applications [307]. Thus, barium tetratitanate ($BaTi_4O_9$) has a twin-type tunnel structure in which the TiO_6 octahedra are not oriented parallel to one another creating a pentagonal prism space. Alkaline metal hexatitanates ($M_2Ti_6O_{13}$; M = Na, K, Rb) are Wadsley–Andersson type structures in which TiO_6 octahedra share an edge at one level in linear groups of three, giving a tunnel structure with rectangular space. The reader should consult the literature for reviews of water photolysis studies using these types of oxides [170, 307]. These materials have been used in powder form in suspensions usually modified with a co-catalyst such as RuO_2 [308–318].

More complex perovskites exist containing two different cations which may occupy either the A or B sites and many of these also have a layered structure. Two main classes of such oxides showing interlamellar activity have been explored for water photolysis: (a) the Dion–Jacobson series of the general formula, $AM_{n\text{-}1}B_nO_{3n+1}$ (e.g., $KCa_2Ti_3O_{10}$) and (b) the Ruddlesden–Popper series of general formula, $A_2M_{n\text{-}1}B_nO_{3n+1}$ (e.g., $K_2La_2Ti_3O_{10}$) [319, 320]. Corresponding niobates also exist as discussed below. Noble metal co-catalysts (e.g., Pt) are loaded onto these photocatalysts by photocatalytic deposition from H_2PtCl_6 (see above). Since the oxide sheets have a net negative charge (that is balanced by the alkali cations), the $PtCl_6^{2-}$ anions are not intercalated in the host lattice [319]. Instead, the Pt sites are formed on the external surfaces of the layered perovskite powder.

In many of these cases with layered oxides, the H^+-exchanged photocatalysts show higher activity toward the HER—a trend rationalized by the easy accessibility of the interlayer space to electron donor species such as methanol [319, 321]. Other aspects such as Ni-loading and pillaring of the interlayer spaces have been discussed [319]. Another type of layered perovskites have been studied with the generic composition, $A_nB_nO_{3n+2}$ (n = 4, 5; A = Ca, Sr, La; B = Nb, Ti) [322]. Unlike the (100)-oriented structures discussed above, the perovskite slabs in these oxides are oriented parallel to the (110) direction. Thus compounds such as $La_2Ti_2O_7$ and $La_4CaTi_5O_{17}$ were examined in terms of their efficacy toward water splitting under UV irradiation [322].

In closing this section, a variety of other ternary oxides (besides the $SrTiO_3$ prototype) have been examined over the years. Table 6 contains a representative listing of these compounds.

8 Tantalates and niobates

We have seen in the preceding section that oxides with MO_6 octahedra can form perovskite structures and this trend also applies to some tantatates and niobates. The perovskite, $KTaO_3$, as well as its Nb-incorporated cousin, $KTa_{0.77}Nb_{0.23}O_3$ were studied early on (1976) in the history of photoelectrolysis of water (see Entry 8 in

Table 5 Studies on the use of $SrTiO_3$ anodes or powders for the photoelectrolysis of water

Entry number	Title of paper	Comments	Reference(s)
1	Photoelectrochemical Reactions at $SrTiO_3$ Single Crystal Electrodes	Cell found to work efficiently even without a pH gradient in the anode and cathode compartments.	[277]
2	Strontium Titanate Photoelectrodes. Efficient Photoassisted Electrolysis of Water at Zero Applied Potential	As above but the water photosplitting driven by light only with no external bias. Photoanode stability also confirmed as in the evolution of H_2 and O_2 in the correct 2:1 stoichiometric ratio.	[278]
3	Photoelectrolysis of Water in Cells with $SrTiO_3$ Anodes	Maximum quantum efficiency at zero bias (10% at $h\nu$ = 3.8eV) found to be ~an order of magnitude higher than TiO_2.	[279]
4	Photoeffects on Semiconductor Ceramic Electrodes	Photoresponse of $SrTiO_3$ found to be better than that of $BaTiO_3$. Unlike the use of single crystals in the above studies (Entries 1–3), polycrystalline electrodes with large area were used.	[280]
5	Surface Photovoltage Experiments on $SrTiO_3$ Electrodes	The role of surface states in mediating charge transfer between electrode and electrolyte elucidated.	[281]
6	Photocatalytic and Photoelectro-chemical Hydrogen Production on Strontium Titanate Single Crystals	Both metal-free and platinized samples studied in aqueous alkaline electrolytes or in the presence of NaOH-coated crystals.	[282]
7	Photocatalytic Decomposition of Water Vapor on an NiO–$SrTiO_3$ Catalyst	A series of studies begun with this particular study which uses powdered photocatalyst. See Entries below.	[283]
8	Visible Light Induced Photo-currents in $SrTiO_3$-$LaCrO_3$ Single-Crystalline Electrodes	Co-doping of La and Cr shifts photoresponse down to 560 nm and strong absorption in the visible range ascribed to $Cr^{3+} \rightarrow Ti^{4+}$ charge transfer.	[284]
9	The Sensitization of $SrTiO_3$ Photo-anodes for Visible Light Irradiation	As in Entry 8 but using the perovskites $LaVO_3$, Sr_2CrNbO_6 and $SrNiNb_2O_9$ as dopants.	[285]
10	The Coloration of Titanates by Transition Metal Ions in View of Solar Energy Applications	–	[286]
11	Evidence of Photodissociation of Water Vapor on Reduced $SrTiO_3$(III) Surfaces in a High Vacuum Environment	First report of photodecomposition of water adsorbed from the gas phase in high vacuum conditions on metal-free, reduced single crystals.	[287]
12	Oxygen Evolution Improvement at a Cr-Doped $SrTiO_3$ Photoanode by a Ru-Oxide Coating	–	[288]
13	Electrochemical Conversion and Storage of Solar Energy	A doped n-$SrTiO_3$ single crystal was combined with a proton-conducting solid electrolyte and a metal hydride allowing for storage of the evolved H_2.	[289]
14	Water Photolysis by UV Irradiation of Rhodium Loaded Strontium Titanate Catalysts. Relation Between Catalytic Activity and Nature of the Deposit from Combined Photolysis and ESCA Studies	Powdered catalysts used and the water photolysis efficiency is found to have a strong pH dependence.	[290]
15	Photocatalytic Decomposition of Liquid Water on a NiO–$SrTiO_3$ Catalyst	As in Entry 7 but for liquid water. Effect of NaOH film (see Entry 6) reproduced for NiO–$SrTiO_3$ powder.	[291]
16	Study of the Photocatalytic Decomposition of Water Vapor over a NiO–$SrTiO_3$ Catalyst	Mechanistic aspects probed by using a closed gas circulation system and IR spectroscopy (see also Entries 7 and 15).	[292]
17	Photoelectrolysis of Water under Visible Light with Doped $SrTiO_3$ Electrodes	Sintered samples used with a variety of dopants (Ru, V, Cr, Ce, Co, Rh).	[293]
18	Mediation by Surface States of the Electroreduction of Photogenerated H_2O_2 and O_2 on n-$SrTiO_3$ in a Photoelectrochemical Cell	Back reactions probed and the role of surface states elucidated.	[294]
19	Photocatalytic Decomposition of Water into H_2 and O_2 over NiO–$SrTiO_3$ Powder. 1. Structure of the Catalyst	Nickel metal also found at the interface of NiO and $SrTiO_3$. See also Entries 7, 15 and 16.	[295]
20	Mechanism of Photocatalytic Decomposition of Water into H_2 and O_2 over NiO–$SrTiO_3$	HER found to occur on the NiO co-catalyst surface while OER takes place on $SrTiO_3$. See also Entries 7, 15, 16 and 19.	[296]

Table 5 continued

Entry number	Title of paper	Comments	Reference(s)
21	Water Photolysis over Metallized $SrTiO_3$ Catalysts	Promoting effect of NaOH not so pronounced as for TiO_2.	[297]
22	Luminescence Spectra from n-TiO_2 and n-$SrTiO_3$ Semiconductor Electrodes and Those Doped with Transition-Metal Oxides As Related with Intermediates of the Photooxidation Reaction of Water	Mechanistic aspects clarified using photo- and electroluminescence measurements.	[298]
23	Photoinduced Surface Reactions on TiO_2 and $SrTiO_3$ Films: Photo-catalytic Oxidation and Photo-induced Hydrophilicity	–	[146]
24	Stoichiometric Water Splitting into H_2 and O_2 using a Mixture of Two Different Photocatalysts and an IO_3/I^- Shuttle Redox Mediator under Visible Light Irradiation	A Z-scheme used using a mixture of Pt-WO_3 and Pt-$SrTiO_3$ photocatalysts. The latter was co-doped with Cr and Ta.	[299]
25	Visible-Light-Response and Photo-catalytic Activities of TiO_2 and $SrTiO_3$ Photocatalysts Co-doped with Antimony and Chromium	The band gap of $SrTiO_3$ shrunk to 2.4 eV by co-doping.	[300]
26	A New Photocatalytic Water Splitting System under Visible Light Irradiation Mimicking a Z-Scheme Mechanism in Photosyn-thesis	See Entry 23 above.	[234]
27	Construction of Z-Scheme Type Heterogeneous Photocatalysis Systems for Water Splitting into H_2 and O_2 under Visible Light Irradiation	A Pt-$SrTiO_3$ doped with Rh is combined with a $BiVO_4$ photocatalyst.	[301]
28	Electrochemical Approach to Evaluate the Mechanism of Photo-catalytic Water Splitting on Oxide Photocatalysts	Cr or Sb co-doped $SrTiO_3$ samples studied amongst others.	[204]
29	H_2 Evolution from a Aqueous Methanol Solution on $SrTiO_3$ Photocatalysts Co-doped with Chromium and Tantalum Ions under Visible Light Irradiation	–	[302]
30	Photocatalytic Activities of Noble Metal Ion Doped $SrTiO_3$ under Visible Light Irradiation	Mn-, Ru-, Rh- and Ir-doped powder samples studied.	[303]
31	Nickel and Either Tantalum or Niobium-Co-doped TiO_2 and $SrTiO_3$ Photocatalysts with Visible-Light Response for H_2 or O_2 Evolution from Aqueous Solutions	Co-doping found to afford higher activity for HER compared with Ni alone.	[210]

Table 6) [257, 326]. Niobium oxides were also considered in early studies aimed at shrinking the large band gaps to values responsive to the visible range of the solar spectrum [333]. Thus in compounds of the type ANb_2O_6 (with A = Ni or Co) we have a conduction band built from d levels of a highly charged, closed-shell transition metal ion (Nb^{5+}) while the highest filled valence band is also cation-derived from the d levels of either Ni^{2+} or Co^{2+} [333]. Thus the main optical transition should be of Ni^{2+} (or Co^{2+}) $\rightarrow$ Nb^{5+} charge-transfer type in the visible region. The ANb_2O_6 oxide has the columbite structure with a $Fe^{2+} \rightarrow Nb^{5+}$ transition featured by a 2.08 eV gap [334]. Families of Bi_2MNbO_7 (M = Al, Ga, In), $A_2B_2O_7$, $InMO_4$ (M = Nb, Ta) compounds all contain the same octahedral TaO_6 or NbO_6 structural units [335].

The parent oxide in these cases can be regarded generically as M_2O_5 (M = Nb or Ta). Table 7 contains a listing of the water photosplitting studies that have appeared on M_2O_5, $ATaO_3$ and more complex tantalates and niobates. Layered perovskite type niobates have the generic formula $A[B_{n-1}Nb_nO_{3n+1}]$ with A = K, Rb, Cs and B = Ca, Sr, Na, Pb, etc. For example, with values of n = 2 and 3, we can derive the structures $A_2M_2O_7$ and $AB_2Nb_3O_{10}$ in Table 7 respectively (Entries 3 and 9). Another series of perovskites has the generic formula: $A_nM_nO_{3n+2}$ with A = Ca, Sr, La and M being either Nb, Ta or Ti. Of course, the simplest compound in this series has the AMO_3 composition as exemplified by $SrTiO_3$ or $KTaO_3$ (see above).

The layered oxides featured in this section and the preceding one have ion-exchange characteristics imparted by the net negative charge residing on the layered sheets. Thus they can assimilate positively charged ions (such as K^+) in the interlamellar spaces. Interestingly, some of these materials (e.g., $K_4Nb_6O_{17}$) have *two* types of interlayer spaces (I and II) which appear alternately [365]. The space ''I'' is easily hydrated even in air while ''II'' is hydrated

Table 6 Other ternary oxides with the general formula, ABO_3,[a] that have been examined from a water photoelectrolysis perspective

Entry number	Oxide	Energy band gap, eV	Comments	Reference(s)
1	$FeTiO_3$[b]	2.16	Unstable with leaching of iron observed during photoelectrolysis.	[323]
2	$YFeO_3$	2.58	N-type semiconductor with an indirect optical transition.	[324]
3	$LuRhO_3$	~2.2	Distorted perovskite structure with p-type semiconductor behavior.	[325]
4	$BaSnO_3$	~3.0	Estimated to be stable toward photoanodic decomposition over a 0.4–14 pH range.	[85]
5	$CaTiO_3$	~3.6	–	[85]
6	$KNbO_3$	~3.1	See next section.	[85]
7	$Ba_{0.8}Ca_{0.2}TiO_3$	~3.25	–	[85]
8	$KTaO_3$	~3.5	Optical to chemical conversion efficiency of ~6% reported. See next section.	[326]
9	$CdSnO_3$	1.77	Band-edges not suitably aligned for HER or OER.	[327]
10	$LaRhO_3$	1.35	See above.	[327]
11	$NiTiO_3$[c]	~1.6	N-type semiconductor crystallizing in the illmenite structure.	[328–330]
12	$LaMnO_3$	~1.1	A p-type semiconductor.	[331, 332]

[a] Not all the oxides in this compilation have the perovskite structure

[b] Other iron titanates: Fe_2TiO_4 (E_g = 2.12 eV) and Fe_2TiO_5 (E_g = 2.18 eV) also examined

[c] ''Band gap'' estimated for the transition from the mid-gap Ni^{2+}(3 d^8) level to the CB. Compound can be regarded as NiO ''doped'' TiO_2

only in a highly humid environment. It is presumed that the NiO co-catalyst exists only in ''I'' such that the HER occurs mainly in this interlayer space. On the other hand, the OER is thought to occur in the interlayer space, II [365].

In general, oxides containing early transition metal cations with d^o electronic configuration such as Ti^{4+}, Nb^{5+} or Ta^{5+} have wide band gaps (> 3.0 eV). In fact Ta_2O_5 has a very high E_g value of ~4.0 eV. Thus, these materials do not perform well under visible light irradiation, and in practical scenarios, would only absorb a small fraction of the solar spectrum. As with TiO_2 and the vast majority of the oxides considered earlier, the ternary (and multinary) oxides, namely the titanates, tantalates and niobates suffer from this same handicap. On the other hand, these materials with smaller E_g values have other problems related to stability, interfacial energetics, poor charge transfer characteristics, etc.

9 Miscellaneous multinary oxides

In this ''catch-all'' section, we mainly discuss the spinel structures with the generic formulas, AB_2O_4 and A_2MO_4. The unit cell of the spinel structure is a large cube, eight times (2 × 2 × 2) the size of a typical face-centered cube [276]. The delafossite-type structure ABO_2, in which the A cation is in linear coordination and the B cation is in octahedral coordination with oxygen, is also discussed. One way to visualize this structure is parallel arrangement of sheets with edge-shared BO_6 octahedral with the A cations occupying the interlayer regions of space. Finally, complex oxides containing V and W are also considered. Table 8 contains a listing of these oxides. It is interesting to note that some of the newer studies (e.g., Entry 4, Table 8) are rooted in early investigations dating back to 1981. Thus, Bi_2WO_6 (as well as $Bi_4Ti_3O_{12}$) were examined [334] within the context of shrinking E_g values of oxide semiconductors. Both these compounds have Bi_2O_2 layers, the former with WO_4 layers (comprised of corner-shared WO_6 octahedra) and the latter with double perovskite layers of composition $Bi_2Ti_3O_{10}$. These structures are distorted from pure tetragonal symmetry. Exfoliation of layered rutile and perovskite tungstates of the generic formula, $HMWO_6$ (M = Nb,Ta) and $H_2W_2O_7$, has been reported [382]. The layered perovskite, $La_2Ti_2O_7$ was sensitized to visible light by Cr or Fe doping and used for photocatalytic hydrogen production from water [383].

10 Semiconductor alloys and mixed semiconductor composites

The distinction between the two classes of materials considered in this section pertains to the presence or absence of mixing at the molecular level. Thus in alloys, solid solutions of two or more semiconductors are formed where the lattice sites are interspersed with the alloy components. Semiconductor alloys, unlike their metallic counterparts, have a much more recent history and their development driver has been mainly optoelectronic (e.g., solid-state la-

Table 7 Studies on tantalate and niobate photocatalysts for the splitting of water.[a]

Entry number	Compound formula	A cation(s)	B cation(s)	Comments	Reference(s)
1	Ta_2O_5	–	–	Both crystallized and mesoporous samples studied and in one case, (Ref. 337), NiO co-catalyst was used.	[336, 337]
2	$ATaO_3$	Li, Na, K	–	Excess alkali cation enhances catalytic activity. Co-catalysts not found to be essential although NiO was also used in addition in some studies.	[338–342]
3	$A(In_{1/3}B_{1/3}M_{1/3})O_3$	Ba	Pb, Sn	Visible light photocatalysts studied with a band gap engineering strategy based on electronegativity of the B metal component.	[343]
4	$A_2M_2O_7$[b]	Sr	–	Have layered perovskite structure. Samples with both Ta and Nb also studied. Strontium niobate compound is ferroelectric at room temperature. In contrast, the tantalum analog is paramagnetic.	[322, 344–346]
5	ANb_2O_6	Ni, Co, Zn	–	See text.	[341, 347]
6	ATa_2O_6	Mg, Ba, Sr	–	Orthorhombic structure used with NiO co-catalyst to enhance photocatalyst activity.	[338, 348]
7	A_2BNbO_6[c]	Sr	Fe	–	[349]
8	$A_3BNb_2O_9$	Sr	Fe	–	[349]
9	$A_4Nb_6O_{17}$	K, Rb	–	Perhaps the most studied of the niobates. NiO co-catalyst used in some cases as was aqueous methanol solution. Composites with CdS also studied.	[350–355]
10	$AB_2Nb_3O_{10}$	K, Rb, Cs	Ca, Sr, Pb	Layered perovskite structure.	[356–359]
11	$A_2B_2Ti_{3-x}Nb_x\ O_{10}$	K, Rb, Cs	La	Partial substitution of Ti with Nb leads to a decrease in the negative charge density of the perovskite sheets.	[360]
12	$A_3Ta_3Si_2O_{13}$	K	–	Pillared structure with TaO_6 pillars linked by Si_2O_7 ditetrahedral units.	[361]
13	$A_2BTa_5O_{15}$	K	Ln	Used with NiO co-catalyst. The Pr and Sm compounds show high activity.	[362]
14	$ATaO_4$	In	–	Crystallizes in the monoclinic wolframite-type structure, like the $FeNbO_4$ compound (see text).	[363]
15	$A_2Nb_4O_{11}$	Cs	–	Structure consists of NbO_6 and NbO_4 octahedra.	[364]

[a] Also see Refs. [66, 365–371]

[b] Belongs to the series A_nMnO_{3n+2} with A = Ca, Sr, La and M = Nb or Ti. The $Sr_2Nb_2O_7$ structure (Entry 3), for example, is the reduced formula of $Sr_4Nb_4O_{14}$ with n = 4 above

[c] The $Sr_{1.9}Fe_{1.1}NbO_6$ compound was also studied here

ser) applications. In mixed semiconductor composites, on the other hand, the semiconductor particles are in *electronic* contact but the composite components do not undergo mixing at the molecular level.

Solid-solutions involving oxide semiconductors that have been examined include TiO_2–MnO_2 [384], ZnO–CdO [384], TiO_2–MO_2 (M = Nb, Ta) [385], TiO_2–In_2O_3 [42], TiO_2–V_2O_5 [41], and Fe_2O_3–Nb_2O_5 [384]. Tungsten-based mixed-metal oxides, $W_nO_mM_x$ (M = Ni, Co, Cu, Zn, Pt, Ru, Rh, Pd and Ag) have been prepared using electrosynthesis and high-throughput (combinatorial) screening [386] but it is not clear how many of these compounds are true alloys (rather than mixtures). An interesting oxide alloy with lamellar structure, $In_2O_3(ZnO)_m$, has been reported [387] with photocatalytic activity for HER in an aqueous methanol and OER in an aqueous $AgNO_3$ solution. This alloy consists of layers of wurtzite-type ZnO slabs interspersed with InO_3 lamella; the band gaps of $In_2O_3(ZnO)_3$ and $In_2O_3(ZnO)_9$ are 2.6 eV and 2.7 eV respectively [387].

The incentive for using mixed semiconductors derives from the possibility of securing interparticle electron transfer and thus mitigates carrier recombination. For example, the conduction band of WO_3 lies at a lower energy (relative to the vacuum reference level) than TiO_2 [388, 389]. Thus, in a TiO_2–WO_3 composite, the photogenerated electrons in TiO_2 are driven to WO_3 before they have an opportunity to recombine with the holes in the TiO_2 particle. Other examples illustrative of this approach were discussed earlier in this chapter and include CdS–TiO_2 [390] and CdS–$K_4Nb_6O_{17}$ [351]. Other examples of mixed semiconductors include TiO_2–$LaCrO_3$ [391] CdS–$LaCrO_3$[332], Fe_2O_3–TiO_2 [392], and Cu_2O–TiO_2 [393]. However, not all these composites have been examined from a water photosplitting perspective. Note that a *bilayer* configuration of the

Table 8 Miscellaneous multinary oxides for the photodecomposition of water

Entry number	Oxide semiconductor(s)	Energy band gap(s)[a], eV	Comments	Reference(s)
1	Cd_2SnO_4, $CdIn_2O_4$ and Cd_2GeO_4	2.12 (indirect), 2.23 (forbidden) and 3.15 (indirect)	Found to be unsuitable as electrodes in photoelectrolysis cells.	[372]
2	$ZnFe_2O_4$	?	HER observed by visible light irradiation of H_2S solution.	[373]
3	$BiVO_4$	2.3	Ag^+ used as electron scavenger and photocatalytic OER observed.	[374]
4	$Bi_2W_2O_9$, Bi_2WO_6 and Bi_3TiNbO_9	3.0, 2.8 and 3.1	Structure consists of perovskite slabs interleaved with Bi_2O_2 layers.	[375]
5	$AgVO_3$, $Ag_4V_2O_7$ and Ag_3VO_4	?	Only Ag_3VO_4 evolves O_2 in aqueous $AgNO_3$ solution (with Ag^+ as electron acceptor) under visible light irradiation.	[376]
6	$ACrO_4$ (A = Sr or Ba)	2.44 and 2.63	The Sr compound shows much lower activity than the Ba counterpart for HER in aqueous methanol.	[377]
7	$CuMnO_2$	1.23	Photocatalytic HER observed in H_2S medium.	[378]
8	$PbWO_4$	?	Has tetragonal structure. Used with RuO_2 co-catalyst for water photosplitting with a Hg–Xe lamp as radiation source.	[379]
9	$CuFeO_2$	?	Photocatalytic water splitting observed under visible light irradiation.	[366, 380, 381]
10	$InVO_4$	1.8 eV	Photocatalytic water splitting with or without NiO in electronic contact observed under visible light irradiation.	[260]

[a] Values for E_g are listed in the order of appearance of the corresponding oxide compound in column 2

two semiconductors is not fundamentally different (at least from an electron transfer perspective) than a suspension containing mixed semiconductor particles (composites) in electronic contact.

11 Photochemical diodes and twin-photosystem configurations for water splitting

Photochemical diodes [53, 394]can be either of the Schottky type, involving a metal and a semiconductor, or a p–n junction type, involving two semiconductors (which can be the same, i.e., a homojunction or different, a heterojunction). Only the latter type is considered in this section involving two irradiated semiconductor/electrolyte interfaces. Thus n-TiO_2 and p-GaP crystal wafers were bonded together (through the rear Ohmic contacts) with conductive Ag epoxy cement [394]. The resultant heterotype p–n photochemical diode was suspended in an acidic aqueous medium and irradiated with simulated sunlight. Evolution of H_2 and O_2 was noted, albeit at a very slow rate [394].

This type of device has been contrasted [394] with a series connection of a photovoltaic p–n junction solar cell and a water electrolyzer. Unlike the latter which is a majority carrier system (i.e., the n-side of the junction is the cathode and the p-side becomes the anode), in a photochemical diode, minority carriers (holes for the n-type and electrons for the p-type) are injected into the electrolyte. This distinction translates to certain advantages in terms of the overall energetics of the solar energy conversion system; see [394] for more details.

Since this original work in 1977, another study has appeared combining p-GaP and n-Fe_2O_3 [63]. Co-catalysts (RuO_2 on the n-Fe_2O_3 surface and Pt on the p-GaP surface) served to enhance H_2 and O_2 evolution from seawater [63]. The p–n photoelectrolysis approach [53, 394] combines a n-type semiconductor photoanode and a p-type semiconductor photocathode in an electrolysis cell (Fig. 2c). The pros and cons of this twin-photosystem approach (which mimicks plant photosynthesis) were enumerated earlier in this article. Table 9 provides a compilation of the semiconductor photocathode and photoanode combinations that have been examined. Combinations involving n-WSe_2, n-$MoSe_2$, n-WS_2, n-TiO_2, p-InP, p-GaP and p-Si semiconductor electrodes have been described [74].

In another interesting variant drawn from early work [396], a semiconductor/redox electrolyte/semiconductor (SES) configuration was deployed as a photoanode. Thus this SES structure consisted of single crystal wafers of n-CdS and n-TiO_2 separated by a thin layer of NaOH, sodium sulfide and sulfur. The inside wall of TiO_2 was coated with Pd to mediate electron transfer between n-TiO_2 and the sulfide-polysulfide redox electrolyte. It was shown [396] that the SES photoanode operated in conjunction with a Pt counter-electrode and 1 M NaOH electrolyte could evolve H_2 and O_2

Table 9 Photoelectrolysis cells using n-type oxide semiconductor photoanodes and p-type semiconductor photocathodes

Entry number	Photoanode	Photocathode	Comments	Reference(s)
1	n-TiO_2	p-GaP	Either 1 N H_2SO_4 or 1 *N* NaOH was employed as electrolyte. The photo-voltage was 0.58 V for the acid and 0.40 V for the base. Deterioration of the cell performance noted.	[93]
3	n-TiO_2	p-GaP	Water splitting noted without need for external bias. See also Entry 1 on the same system.	[53]
4	n-TiO_2	p-CdTe	–	[395]
5	n-TiO_2	p-GaP	–	[395]
6	n-$SrTiO_3$	p-CdTe	–	[395]
7	n-$SrTiO_3$	p-GaP	Best performance among the four combinations tested. (See Entries 4–6 above.)	[395]

without external bias. The OER occurs on the n-TiO_2 surface and HER occurs on the Pt counterelectrode surface.

12 Concluding remarks

The use of irradiated oxide semiconductor-liquid interfaces for hydrogen generation is now a mature field of research. Indeed, impressive results have been obtained at the laboratory scale over the past three decades and a myriad of new oxides are being continually discovered. On the other hand, much needs to be done to improve the H_2 generation efficiencies. The photoelectrolysis process must be engineered and scaled up for routine practical use. In this regard, oxide semiconductors appear to be particularly promising, especially from an environmental and process economics perspective. While interesting chemistry, physics, and materials science discoveries will continue to push this field forward, in the author's opinion two types of R&D will be crucial: the use of combinatorial, high throughput methods for photocatalyst development and innovations in reactor/process engineering once efficiencies at the laboratory scale have been optimized at a *routinely attainable* ~10% benchmark. Only then will the long sought after goal of efficiently making H_2 from sunlight and water using this approach be realised.

Acknowledgments Partial support from the U. S. Department of Energy (Basic Energy Sciences) for the author's research on photoelectrochemical solar energy conversion is gratefully acknowledged. Professors B. A. Parkinson, J. Augustynski, C. A. Grimes and M. Matsumura kindly provided reprints/preprints. Dr. C. R. Chenthamarakshan and Ms. Gloria Madden are thanked for assistance in literature research and manuscript preparation. Finally, three anonymous reviewers are thanked for constructive criticisms of an earlier manuscript version, and for alerting the author to Refs. [171, 187, 218, 223], [255, 260, 318, 343], and [383].

References

1. Grätzel M (eds) (1983) Energy resources through photochemistry and catalysis. Academic Press, NY
2. Pleskov YV, Gurevich YY (1986) Semiconductor photoelectrochemistry. Consultants Bureau, NY and London
3. Hamnett A (1987) Comprehensive chemical kinetics, vol. 27, Electrode kinetics: reactions. Compton RG (ed) Ch. 2, p. 61, Elsevier, Amsterdam
4. Finklea HO (eds) (1988) Semiconductor electrodes. Elsevier, Amsterdam
5. Peter LM, Vanmaelkelbergh D (1999) In: Alkire RC and Kolb DM (eds) Advances in electrochemical science and engineering. Wiley-VCH, Weinheim 6:77
6. Memming R (2001) Semiconductor electrochemistry. Wiley-VCH, Weinheim
7. Licht S (2001) editor, Semiconductor electrodes and photoelectrochemistry – Encyclopedia of electrochemistry, Wiley-VCH, Weinheim Vol. 6
8. Archer MD (1975) J Appl Electrochem 5:17
9. Rajeshwar K, Singh P, DuBow J (1978) Electrochim Acta 23:1117
10. Wilson RH (1980) CRC Crit Rev Mater Sci 10:1
11. Heller A (1981) Acc Chem Res 14:154
12. Grätzel M (1981) Acc Chem Res 14:376
13. Parkinson B (1984) Acc Chem Res 17:31
14. Rajeshwar K (1985) J Appl Electrochem 15:1
15. Koval CA, Howard JN (1992) Chem Rev 92:411
16. Kumar A, Wilisch WCA, Lewis NS (1993) Crit Rev Solid State Mater Sci 18:327
17. Tan MX, Laibinis PE, Nguyen ST, Kesselman JM, Stanton CE, Lewis NS (1994) Prog Inorg Chem 41:21
18. Bard AJ, Fox MA (1995) Acc Chem Res 28:141
19. Nozik AJ, Memming R (1996) J Phys Chem 100:13061
20. Lewis NS (1998) J Phys Chem 102:4843
21. Lewis NS (2001) J Electroanal Chem 508:1
22. Grätzel M (2001) Nature 414:338
23. Brattain WH, Garrett CGB (1955) Bell Syst Tech J 34:129
24. Dewald JF (1960) Bell Syst Tech J 39:615
25. Turner DR (1961) J Electrochem Soc 103:252
26. Dewald JF (1961) J Phys Chem Solids 14:155
27. Boddy PJ, Brattain W (1962) J Electrochem Soc 109:1053
28. Boddy PJ (1968) J Electrochem Soc 115:199
29. Fujishima A, Honda K (1971) Bull Chem Soc Jpn 44:1148
30. Fujishima A, Honda K (1972) Nature 238:37
31. Fujishima A, Kohayakawa K, Honda K (1975) Bull Chem Soc Jpn 48:1041
32. Fujishima A, Kohayakawa K, Honda K (1975) J Electrochem Soc 122:1487
33. Watanabe T, Fujishima A, Honda K in Ref 1, p 359
34. Smith RA (1964) Semiconductors. Cambridge At the University Press, Cambridge, England

35. Cox PA (1987) The electronic structure and chemistry of solids. Oxford University Press, Oxford, England
36. Ellis AB, Geselbracht MJ, Johnson BJ, Lisensky GC, Robinson WR (1993) Teaching general chemistry – A materials science companion, Chapter 7. American Chemical Society, Washington, DC, p 187
37. Meissner D, Memming R, Kastening B (1983) Chem Phys Lett 96:34
38. Jackowska K, Tien HT (1988) Solar Cells 23:147
39. Tien HT, Chen JW (1990) Int J Hydrogen Energy 15:563
40. Kondapaneni SC, Singh D, Srivastava ON (1992) J Phys Chem 96:8094
41. Karn RK, Misra M, Srivastava ON (2000) Int J Hydrogen Energy 25:407
42. Srivastava ON, Karn RK, Misra M (2000) Int J Hydrogen Energy 25:495
43. Hara M, Mallouk TE (2000) Chem Commun 1903
44. Review: Yagi M, Kaneko M (2001) Chem Rev 101:21
45. Kiwi J, Borgarello E, Pelizzetti E, Visca M, Grätzel M (1980) Angew Chem Int Ed Engl 19:646
46. Borgarello E, Kivi J, Pelizzetti E, Visca M, Grätzel M (1981) Nature 289:158
47. Pichat P, Hermann JM, Disdier J, Bourbon H, Mozzanega MN (1981) Nov J Chim 5:627
48. Degani Y, Willner I (1983) J Chem Soc, Chem Commun 710
49. Frank AJ, Willner I, Goren Z, Degani Y (1987) J Am Chem Soc 109:3568
50. Maruthamuthu P, Gurunathan K, Subramanian E, Sastri MVC (1994) Int J Hydrogen Energy 19:889
51. Gurunathan K, Maruthamuthu P, Sastri MVC (1997) Int J Hydrogen Energy 22:57
52. Shiroishi H, Nukaga M, Yamashita S, Kaneko M (2002) Chem Lett 488
53. Nozik AJ (1976) Appl Phys Lett 29:150
54. Licht S (2001) J Phys Chem 105:6281
55. Bolton JR (1996) Solar Energy 57:37
56. Bilgen E (2001) Energy Conversion Manage 42:1047
57. Khaselev O, Bansal A, Turner JA (2001) Int J Hydrogen Energy 26:127
58. Turner JA (1998) Science 280:425
59. Kocha SS, Montgomery D, Peterson MW, Turner JA (1998) Solar Energy Mater Solar Cells 52:389
60. Gao X, Kocha SS, Frank AJ, Turner JA (1999) Int J Hydrogen Energy 24:319
61. Shukla PK, Karn RK, Singh AK, Srivastava ON (2002) Int J Hydrogen Energy 27:135
62. Khaselev O, Turner JA (1998) Science 280:425
63. Mettee H, Otvos JW, Calvin M (1981) Solar Energy Mater 4:443
64. Fonash SJ (1981) Solar Cell Device Physics. Academic Press, San Diego
65. Heller A (1984) Science 223:1141
66. Rauh RD, Buzby JM, Reise TF, Alkaitis SA (1979) J Phys Chem 83:2221
67. Rajeshwar K, Ibanez JB (1995) J Chem Educ 72:1044
68. Kraeutler B, Bard AJ (1978) J Am Chem Soc 100:4317
69. Kraeutler B, Bard AJ (1978) J Am Chem Soc 100:5985
70. Heller A in Ref. 1, Chapter 12, p. 385
71. Wrighton MS (1983) J Chem Educ 60:877
72. Natan MJ, Wrighton MS (1989) Prog Inorg Chem 37:391
73. Wrighton MS (1986) Science 231:32
74. Fornarini L, Nozik AJ, Parkinson BA (1984) J Phys Chem 88:3238
75. Archer MD, Bolton JR (1990) J Phys Chem 94:8028
76. Bockris J'OM, Murphy OJ (1982–83) Appl Phys Commun 2:203
77. Zafir M, Ulman M, Zuckerman Y, Halmann M (1983) J Electroanal Chem 159:373
78. Bak T, Nowotny J, Rekas M, Sorrell CC (2002) Int J Hydrogen Energy 27:991
79. Weber MF, Dignam MJ (1984) J Electrochem Soc 131:1258
80. Gerischer H (1979) In: Seraphin BO (ed) Solar energy conversion. Springer, Berlin, p 115
81. Review: Rajeshwar K, de Tacconi NR, Chenthamarakshan CR (2004) Curr Opinion Solid State Mater Sci 8:173; see also references therein
82. For example: Lincot D, Froment M, Cachet H (1999) In: Alkire RC, Kolb DM (eds) Advances in electrochemical science and engineering, vol 6. Wiley-VCH, Weinheim, p 165
83. Review: Rao CNR (1993) Mater Sci Eng B 18:1
84. Kung HH, Jarrett HS, Sleight AW, Feretti A (1977) J Appl Phys 48:2463
85. Scaife DE (1980) Solar Energy 25:41
86. Goodenough JB, Hamnett A, Dare-Edwards MP, Campet G, Wright RD (1980) Surf Sci 101:531
87. For example: Egerton TA, King CJ (1979) J Oil Col Chem Assoc 62:386
88. Carey JH, Laurence J, Tosine HM (1976) Bull Environ Contamination Toxicol 16:697
89. Carey JH, Oliver G (1980) Water Poll Res J Canada 15:157
90. Ohnishi T, Nakato Y, Tsubomura H (1975) Ber Bunsen-Ges Phys Chem 89:523
91. Nozik AJ (1975) Nature 257:383
92. Mavroides JG, Tcherner DI, Kafalas JA, Kolesar DF (1975) Mater Res Bull 10:1023
93. Yoneyama H, Sakamoto H, Tamura H (1975) Electrochim Acta 20:341
94. Wrighton MS, Ginley DS, Wolczanski PT, Ellis AB, Morse DL, Linz A (1975) Proc Nat Acad Sci USA 72:1518
95. Hardee KL, Bard AJ (1975) J Electrochem Soc 122:739
96. Bockris JO'M, Uosaki K (1976) Energy 1:143
97. Morisaki H, Watanabe T, Iwase M, Yazawa K (1976) Appl Phys Lett 29:338
98. Gissler W, Lensi PL, Pizzini S (1976) J Appl Electrochem 6:9
99. Carey JH, Oliver BG (1976) Nature 259:554
100. Houlihan JF, Madacsi DP, Walsh EJ (1976) Mater Res Bull 11:1191
101. Desplat JL (1976) J Appl Phys 47:5102
102. Augustynski J, Hinden J, Stalder C (1977) J Electrochem Soc 124:1063
103. Ghosh AK, Maruska HP (1977) J Electrochem Soc 124:1516
104. Nobe K, Bauerle GL, Brown M (1977) J Appl Electrochem 7:379
105. Tamura H, Yoneyama H, Iwakura C, Sakamoto H, Murakami S (1977) J Electroanal Chem 80:357
106. Morisaki H, Hariya M, Yazawa K (1977) Appl Phys Lett 30:7
107. Tamura H, Yoneyama H, Iwakawa C, Murai T (1977) Bull Chem Soc Jpn 50:753
108. Haneman D, Holmes P (1979) Solar Energy Materials 1:233
109. Clechet P, Martelet C, Martin JR, Oliver R (1979) Electrochim Acta 24:457
110. Sato S, White JM (1980) Chem Phys Lett 72:83
111. Kawai T, Sakata T (1980) Chem Phys Lett 72:87 (See also references therein.)
112. Julião JF, Decker F, Abramovich M (1980) J Electrochem Soc 127:2264
113. Kowalski JM, Johnson KH, Tuller HL (1980) J Electrochem Soc 127:1969
114. Rao MV, Rajeshwar K, Pai Verneker VR, DuBow J (1980) J Phys Chem 84:1987
115. Salvador P (1980) J Electrochem Soc 128:1895

116. Sato S, White JM (1981) J Catal 69:128
117. Mills A, Porter G (1982) J Chem Soc, Faraday Trans I 78:3659
118. Oosawa Y (1982) J Chem Soc Chem Commun 221
119. Kiwi J, Grätzel M (1984). J Phys Chem 88:1302 (See also references therein)
120. Furlong DN, Wells D, Sasse WHF (1985) J Phys Chem 89:626
121. Kobayashi T, Yoneyama H, Tamura H (1981) J Electroanal Chem 124:179
122. Kobayashi T, Yoneyama H, Tamura H (1981) J Electroanal Chem 122:133
123. Salvador P (1982) Solar Energy Materials 6:241
124. Nakato Y, Tsumura A, Tsubomura H (1982) Chem Phys Lett 85:387
125. Kobayashi T, Yoneyama H, Tamura H (1982) J Electroanal Chem 138:105
126. Nakato Y, Tsumura A, Tsubomura H (1983) J Phys Chem 87:2402
127. Salvador P, Decker F (1984) J Phys Chem 88:6116
128. Oosawa Y, Grätzel M (1984) J Chem Soc Chem Commun 1629
129. Brown GT, Darwent JR (1984) J Phys Chem 88:4955
130. Abrahams J, Davidson RS, Morrison CL (1985) J Photochem 29:353
131. Ulmann M, de Tacconi NR, Augustynski J (1986) J Phys Chem 90:6523
132. Munuera G, Gonzalez-Elipe GR, Fernandez A, Malet P, Espinos JP (1989) J Chem Soc Faraday Trans I 85:1279
133. Peterson MW, Turner JA, Nozik AJ (1991) J Phys Chem 95:221
134. Augustynski J (1993) Electrochim Acta 38:43
135. Riegel G, Bolton JR (1995) J Phys Chem 99:4215
136. Nakato Y, Akanuma H, Shimizu JI, Magari Y (1995) J Electroanal Chem 396:35
137. Sun J, Bolton JR (1996) J Phys Chem 100:4127
138. Bahnemann DW, Hilgendorff M, Memming R (1997) J Phys Chem B 101:4265
139. Connor PA, Dobson KD, McQuillan AJ (1999) Langmuir 15:2402
140. Hirakawa T, Nakaoka Y, Nishino J, Nosaka Y (1999) J Phys Chem B 103:4399
141. Boschloo G, Fitzmaurice D (1999) J Phys Chem B 103:2228
142. Boschloo G, Fitzmaurice D (1999) J Phys Chem B 103:7860
143. Szczepankiewicz SH, Colussi AJ, Hoffmann MR (2000) J Phys Chem B 104:9842
144. Ishibashi KI, Fujishima A, Watanabe T, Hashimoto K (2000) J Phys Chem B 104:4934
145. Tsujiko A, Kisumi T, Magari Y, Murakoshi K, Nakato Y (2000) J Phys Chem B 104:4873
146. Miyauchi M, Nakajima A, Fujishima A, Hashimoto K, Watanabe T (2000) Chem Mater 12:3
147. Yamakata A, Ishibashi T, Onishi H (2001) J Phys Chem B 105:7258
148. Li X, Chen C, Zhao J (2001) Langmuir 174118
149. Ohno T, Sarukawa K, Matsumura M (2001) J Phys Chem B 105:2417
150. Szczepankiewicz SH, Moss JA, Hoffmann MR (2002) J Phys Chem B 106:2922
151. Fabregat-Santiago F, Garcia-Belmonte G, Bisquert J, Zaban A, Salvador P (2002) J Phys Chem B 106:334
152. Somasundaram S, Tacconi N, Chenthamarakshan CR, Rajeshwar K, de Tacconi NR (2005) J Electroanal Chem 577:167
153. Hurum DC, Gray KA, Rajh T, Thurnauer MC (2005) J Phys Chem B 109:977
154. Stalder C, Augustynski J (1979) J Electrochem Soc 126:2007
155. Houlihan JF, Armitage DB, Hoovler T, Bonaquist D, Mullay LN (1978) Mater Res Bull 13:1205
156. Monnier A, Augustynski J (1980) J Electrochem Soc 127:1576
157. Salvador P (1980) Mater Res Bull 151287
158. Matsumoto Y, Kurimoto J, Shimizu T, Sato E (1981) J Electrochem Soc 128:1090
159. Karakitsou KE, Verykios XE (1993) J Phys Chem 97:1184. (See also references therein.)
160. Zhang Z, Wang CC, Zakaria R, Ying JY (1998) J Phys Chem B 102:10871
161. Maruska HP, Ghosh AK (1978) Solar Energy 20:1443
162. Hoffman MR, Martin ST, Choi W, Bahnemann DW (1995) Chem Rev 95:69
163. Linsebigler AL, Lu G, Yates Jr JT (1996) Chem Rev 95:735
164. DiPaola A, Marci G, Palmesano L, Schiavello M, Uosaki K, Ikeda S, Ohtani B (2002) J Phys Chem B 106:637
165. Zang L, Macyk W, Lange C, Maier WF, Antonius C, Meissner D, Kisch H (2000) Chem Eur J 6:379
166. Stathatos E, Lianos P, Falaras P, Siokou A (2000) Langmuir 16:2398
167. Stathatos E, Petrova T, Lianos P (2001) Langmuir 17:5025
168. Nakamura I, Negishi N, Kutsuna S, Ihara T, Sugihara S, Takeuchi K (2000) J Mol Catal A Chem 161:205
169. Anpo M, Takeuchi M, Ikeue K, Dohshi S (2002) Curr Opinion Solid State Mater Sci 6:381 (See also references therein)
170. Anpo M (2002) In: Kaneko M, Okura I (eds) Photocatalysis. Kodansha/Springer, Berlin, Chapter 10, p 175
171. Kim S, Hwang SJ, Choi W (2005) J Phys Chem B 109:24260
172. Asahi R, Morikawa T, Ohwaki T, Aoki K, Taga Y (2001) Science 293:269
173. Yamaki T, Sumita T, Yamamoto S (2002) J Mater Sci Lett 21:33
174. Umebayashi T, Yamaki T, Itoh H, Asai K (2002) Appl Phys Lett 81:454
175. Khan SUM, Al-Shahry M, Ingler Jr WB (2002) Science 297:2243
176. Fujishima A (2003) Science 301:1673a
177. Hägglund C, Grätzel M, Kasemo B (2003) Science 301:1673b
178. Lackner KS (2003) Science 301:1673c
179. Sakthivel S, Kisch H (2003) Angew Chem Int Ed 42:4908
180. Irie H, Watanabe Y, Hashimoto K (2003) Chem Lett 32:772
181. Irie H, Watanabe Y, Hashimoto K (2003) J Phys Chem B 107:5483
182. Umebayashi T, Yamaki T, Tanaka S, Arai K (2003) Chem Lett 32:330
183. Irie H, Washizuka S, Yoshino N, Hashimoto K (2003) Chem Commun 1298
184. Noworyta K, Augustynski J (2004) Electrochem Solid-State Lett 7:E31
185. Torres GR, Lindgren T, Lu J, Granqvist CG, Lindquist SE (2004) J Phys Chem B 108:5995
186. Sakatani Y, Ando H, Okusako K, Koike H, Nunoshige J, Takata T, Kondo JN, Hara M, Domen K (2004) J Mater Sci 19:2100
187. Park JH, Kim S, Bard AJ (2006) Nano Lett 6:24
188. Hattori A, Yamamoto M, Tada H, Ito S (1998) Chem Lett 707
189. Inoue Y, Okamura M, Sato K (1985) J Phys Chem 89:5184
190. Kudo A, Domen K, Maruya K, Onishi T (1988) Bull Chem Soc Jpn 61:1535
191. Yamaguchi K, Sato S (1985) J Chem Soc Faraday Trans I 81:1237
192. Sayama K, Arakawa H (1992) J Chem Soc Chem Commun 150
193. Sayama K, Arakawa H (1997) J Chem Soc, Faraday Trans 931647
194. Arakawa H, Sayama K (2000) Res Chem Intermed 26:145
195. Kudo A, Domen K, Maruya K, Onishi T (1989) Chem Phys Lett 133:517
196. Pleskov YuV, Krotova MD (1993) Electrochim Acta 38:107
197. Ohno T, Haga D, Fujihara K, Kaizaki K, Matsumura M (1997) J Phys Chem B 101:6415

198. Fujihara K, Ohno T, Matsumura M (1998) J Chem Soc Faraday Trans 94:3705
199. Abe T, Suzuki E, Nagoshi K, Miyashita K, Kaneko M (1999) J Phys Chem B 103:1119
200. Ohno T, Sarukawa K, Matsumura M (2001) J Phys Chem B 105:2417
201. Abe R, Sayama K, Domen K, Arakawa H, Chem Phys Lett 344:339
202. Kato H, Kudo A (2002) J Phys Chem B 106:5029
203. Abe R, Sayama K, Arakawa H (2003) Chem Phys Lett 379:230
204. Matsumoto Y, Unal U, Tanaka N, Kudo A, Kato H (2004) J Solid State Chem 177:4205
205. Mor GK, Shankar K, Varghese OK, Grimes CA (2004) J Mater Res 19:2989
206. Mor GK, Shankar K, Paulose M, Varghese OK, Grimes CA (2005) Nano Lett 5:191
207. Varghese OK, Paulose M, Shankar K, Mor GK, Grimes CA (2005) J Nanosci Nanotechnol 5:1158
208. Shankar K, Paulose M, Mor GK, Varghese OK, Grimes CA (2005) J Phys D Appl Phys 38:3543
209. Mor GK, Varghese OK, Paulose M, Shankar K, Grimes CA (2006) Solar Energy Mater Solar Cells 90:2011
210. Riishiro R, Kato H, Kudo A (2005) Phys Chem Chem Phys 7:2241
211. Sato S (2002) In: Kaneko M, Okura I (eds) Photocatalysis. Kodansha/Springer, Berlin, Chapter 13, p 223
212. Tabata S, Nishida N, Masaka Y, Tabata K (1995) Catal Lett 34:245
213. Sato S, White JM (1980) J Am Chem Soc 102:7206
214. Arakawa H, Sayama K (2002) In: Kaneko M, Okura I (eds) Photocatalysis. Kodansha/Springer, Berlin, Chapter 14, p 235
215. Perkins CL, Henderson MA, McCready DE, Herman GS (2001) J Phys Chem B 105:595
216. Sato S (1985) Catal J 92:11
217. Ohno T, Matsumura M (2002) In: Kaneko M, Okura I (eds) Photocatalysis. Kodansha/Springer, Berlin, Chapter 17, p 279
218. Grätzel M (2005) Chem Lett 34:8
219. Nowotny MK, Bak T, Nowotny J (2006) J Phys Chem B 110:16270
220. Nowotny MK, Bak T, Nowotny J (2006) J Phys Chem B 110:16283
221. Nowotny MK, Bak T, Nowotny J (2006) J Phys Chem B 110:16292
222. Nowotny MK, Bak T, Nowotny J (2006) J Phys Chem B 110:16302
223. Stewart SJ, Fernandez-Garcia M, Belvor C, Mun BS, Requejo FG (2006) J Phys Chem B 110:16482
224. Butler MA, Nasby RD, Quinn RK (1976) Solid State Commun 19:1011
225. Butler MA (1977) J Appl Phys 48:1914
226. Derrington CE, Godek WS, Castro CA, Wold A (1978) Inorg Chem 17:977
227. Darwent JR, Mills A (1982) J Chem Soc Faraday Trans 278:359
228. Erbs W, DeSilvestro J, Borgarello E, Gräzel M (1984) J Phys Chem 88:4001
229. Maruthamuthu P, Ashok Kumar M, Gurunathan K, Subramanian E, Sastri MVC (1989) Int J Hydrogen Energy 14:525
230. Santato C, Ulmann M, Augustynski J (2001) Adv Mater 13:511
231. Wang H, Lindgren T, He J, Hagfeldt A, Lindquist SE (2000) J Phys Chem B 104:5686
232. Santato C, Ulmann M, Augustynski J (2001) J Phys Chem B 105:936
233. Santato C, Odziemkowski M, Ulmann M, Augustynski J (2001) J Am Chem Soc 123:10639
234. Sayama K, Mukasa K, Abe R, Abe Y, Arakawa H (2002) J Photochem Photobiol A Chem 148:71
235. Hwang DW, Kim J, Park TJ, Lee JS (2002) Catal Lett 80:53
236. Khan SUM, Akikusa J (1999) J Phys Chem B 103:7184
237. Hardee KL, Bard AJ (1976) J Electrochem Soc 123:1024
238. Quinn RK, Nasby RD, Baughman RJ (1976) Mater Res Bull 11:1011
239. Hardee KL, Bard AJ (1977) J Electrochem Soc 124:215
240. Yeh LSR, Hackerman N (1977) J Electrochem Soc 124:833
241. Kennedy JH, Frese Jr KW (1978) J Electrochem Soc 125:709
242. Leygraf C, Hendewerk M, Somorjai GA (1982) J Phys Chem 86:4484
243. Shinar R, Kennedy JH (1982) Solar Energy Materials 6:323 (See also references therein.)
244. Leygraf C, Hendewerk M, Somorjai GA (1982) Proc Natl Acad Sci USA 79:5739
245. Leygraf C, Hendewerk M, Somorjai GA (1983) J Solid State Chem 48:357
246. Dare-Edwards MP, Goodenough JB, Hamnett A, Trevellick PR (1983) J Chem Soc Faraday Trans I 79:2027
247. Gurunathan K, Maruthamuthu P (1995) Int J Hydrogen Energy 20:287
248. Watanabe A, Kozuka H (2003) J Phys Chem B 107:12713
249. Lindgren T, Wang H, Beermann N, Vayssieres L, Hagfeldt A, Lindquist SE (2002) Solar Energy Mater Solar Cells 71:231
250. Sartoretti CJ, Ulmann M, Alexander BD, Augustynski J, Weiden-Kaff A (2003) Chem Phys Lett 376:194
251. Ingler Jr. WB, Khan SUM (2004) Thin Solid Films 461:301
252. Ingler Jr. WB, Baltrus JP, Khan SUM (2004) J Am Chem Soc 126:10238
253. Sartoretti CJ, Alexander BD, Solarska R, Rutkawska IA, Augustynski J, Cerny R (2005) J Phys Chem B 109:13685
254. Woodhouse M, Herman GS, Parkinson BA (2005) Chem Mater 17:4318
255. Cesar I, Kay A, Gonzalez-Martinez JA, Grätzel M (2006) J Am Chem Soc 128:4582
256. Wrighton MS, Morse DL, Ellis AB, Ginley DS, Abrahamson HB (1976) J Am Chem Soc 98:44
257. Bolts JM, Wrighton MS (1976) J Phys Chem 80:2641
258. Dare-Edwards MP, Goodenough JB, Hamnett A, Nicholson ND (1981) J Chem Soc, Faraday Trans II 77:643
259. Koffyberg FP, Benko FA (1981) J Electrochem Soc 128:2476
260. Lin HY, Chen YF, Chen YW (2007) Int J Hyrogen Energy 32:86
261. Harriman A (1983) J Chem Soc Faraday Trans I 79:2875
262. Dare-Edwards MP, Goodenough JB, Hamnett A, Katty A (1984) Mater Res Bull 19:435
263. Hara M, Kondo T, Komoda M, Ikeda S, Shinohara K, Tanaka A, Kondo JN, Domen K (1998) Chem Commun 357
264. de Jongh PE, Vanmaekelbergh D, Kelly JJ (1999) Chem Commun 1069
265. Koffyberg FP, Benko FA (1982) J Appl Phys 53:1173
266. Maruthamuthu P, Gurunathan K, Subramanian E, Sastri MVC (1993) Int J Hydrogen Energy 18:9
267. Maruthamuthu P, Gurunathan K, Subramanian E, Sastri MVC (1994) Int J Hydrogen Energy 19:889
268. Gurunathan K (2004) Int J Hydrogen Energy 29:933
269. Hodes G, Cahen D, Manassen J (1976) Nature 260:312
270. Duret A, Grätzel M (2005) J Phys Chem B 109:17184
271. Somasundaram S, de Tacconi NR, Chenthamarakshan CR, Rajeshwar K (submitted)
272. Mbindyo JKN, Ahmadi MF, Rusling JF (1997) J Electrochem Soc 144:3153
273. Soler L, Maćanas J, Muňoz M, Casado J (2006) Int J Hydrogen Energy 31:129
274. Butler MA, Ginley DS (1978) J Electrochem Soc 125:228
275. Wells AF (1962) Structural inorganic chemistry, 3rd edn. Oxford University Press, Clarendon
276. West AR (2000) Basic solid state chemistry, 2nd edn. John Wiley & Sons, Chichester

277. Watanabe T, Fujishima A, Honda K (1976) Bull Chem Soc Jpn 49:355
278. Wrighton MS, Ellis AB, Wolczanski PT, Morse DL, Abrahamson HB, Ginley DS (1976) J Am Chem Soc 98:2774
279. Mavroides JG, Kafalas JA, Kolesar DF (1976) Appl Phys Lett 28:241
280. Okuda M, Yoshida K, Tanaka N (1976) Japan J Appl Phys 15:1599
281. Mavroides JG, Kolesar DF (1978) J Vac Sci Technol 15:538
282. Wagner FT, Somorjai GA (1980) J Am Chem Soc 102:5494
283. Domen K, Naito S, Soma M, Onishi T, Tamaru K (1980) J Chem Soc Chem Commun 543
284. Mackor A, Blasse G (1981) Chem Phys Lett 77:6
285. de Korte PHM, de Haart LGJ, Lam RUE 't, Blasse G (1981) Solid State Commun 38:213
286. Blasse G, de Korte PHM, Mackor A (1981) J Inorg Nucl Chem 43:1499
287. Ferrer S, Somorjai GA (1981) J Phys Chem 85:1464
288. Salvador P, Fernandez VM, Gutierrez C (1982) Solar Energy Mater 7:323
289. Schoonman J (1982) Ber Bunsenges Phys Chem 86:660
290. Lehn JM, Sauvage JP, Ziessel R, Hilaire L (1982) Isr J Chem 22:168
291. Domen K, Naito S, Onishi T, Tamaru K (1982) Chem Phys Lett 92:433
292. Domen K, Naito S, Onishi T, Tamaru K, Soma M (1982) J Phys Chem 86:3657
293. Matsumura M, Hiramoto M, Tsubomura H (1983) J Electrochem Soc 130:326
294. Salvador P, Gutierrez C (1983) Surf Sci 124:398
295. Domen K, Kudo A, Onishi T, Kosugi N, Kuroda H (1986) J Phys Chem 90:292
296. Domen K, Kudo A, Onishi T (1986) J Catal 102:92
297. Yamaguchi K, Sato S (1986) Nov J Chem 10:217
298. Nakato Y, Ogawa H, Morita K, Tsubomura H (1986) J Phys Chem 90:6210
299. Sayama K, Mukasa K, Abe R, Abe Y, Arakawa H (2001) Chem Commun 2416
300. Kato H, Kudo A (2002) J Phys Chem B 106:5029
301. Kato H, Hori M, Konta R, Shimodaira Y, Kudo A (2004) Chem Lett 33:1348
302. Ishii T, Kato H, Kudo A (2004) J Photochem Photobiol A Chem 163:181
303. Konta R, Ishii T, Kato H, Kudo A (2004) J Phys Chem B 108:8992
304. Schleich DM, Derrington C, Godek W, Weisberg D, Wold A (1977) Mater Res Bull 12:321
305. Nasby RD, Quinn RK (1976) Mater Res Bull 11:985
306. Kennedy JH, Frese Jr KW (1976) J Electrochem Soc 123:1683
307. Inoue Y (2002) In: Kaneko M, Okura I (eds) Photocatalysis. Kodansha/Springer, Berlin, Chapter 15, p 249
308. Shibata M, Kudo A, Tanaka A, Domen K, Maruya K, Onishi T (1987) Chem Lett 1017
309. Inoue Y, Kubokawa T, Sato K (1990) J Chem Soc, Chem Commun 1298
310. Inoue Y, Kubokawa T, Sato K (1991) J Phys Chem 95:4059
311. Inoue Y, Niiyama T, Asai Y, Sato K (1992) J Chem Soc Chem Commun 579
312. Kohno M, Oyura S, Inoue Y (1996) J Mater Chem 61921
313. Takata T, Furumi Y, Shinohara K, Tanaka A, Hara M, Kondo JN, Domen K (1997) Chem Mater 9:1063
314. Kohno M, Ogura S, Sato K, Inoue Y (1997) J Chem Soc Faraday Trans 93:2433
315. Ikeda S, Hara M, Kondo JN, Domen K, Takahashi H, Okuho T, Kakihana M (1998) J Mater Res 13:852
316. Ogura S, Kohno M, Sato K, Inoue Y (1998) J Mater Chem 8:2335
317. Kohno M, Kaneko T, Ogura S, Sato K, Inoue Y (1998) J Chem Soc Faraday Trans 94:89
318. Sato J, Saito N, Nishiyama N, Inoue Y (2003) J Phys Chem B 107:7965
319. Domen K (2002) In: Kaneko M, Okura I (eds) Photocatalysis, Kodansha/Springer, Berlin, Chapter 16, p 261
320. Schaak RE, Mallouk TE (2000) Chem Mater 12:3427
321. Hoertz PG, Mallouk TE (2005) Inorg Chem 44:6828
322. Kim HG, Hwang DW, Kim J, Kim YG, Lee JS (1999) Chem Commun 1077 (See also references therein.)
323. Ginley DS, Butler MA (1977) J Appl Phys 48:2019
324. Butler MA, Ginley DS, Eibschutz M (1977) J Appl Phys 48:3070
325. Jarrett HS, Sleight AW, Kung HH, Gillson JL (1980) J Appl Phys 51:3916
326. Ellis AB, Kaiser SW, Wrighton MS (1976) J Phys Chem 80:1325
327. Yoneyama H, Ohkubo T, Tamura H (1981) Bull Chem Soc Jpn 54:404
328. Salvador P, Gutierrez C, Goodenough JB (1982) Appl Phys Lett 40:188
329. Gutierrez C, Salvador P (1982) J Electroanal Chem 134:325
330. Salvador P, Gutierrez C, Goodenough JB (1982) J Appl Phys 53:7003
331. Lianos P, Thomas JK (1986) Chem Phys Lett 125:299
332. Kida T, Guan G, Minami Y, Ma T, Yoshida A (2003) J Mater Chem 13:1186
333. Blasse G, Dirksen GJ, de Korte PHM (1981) Mater Res Bull 16:991
334. Koenitzer J, Khazai B, Hormadaly J, Kershaw R, Dwight K, Wold A (1980) J Solid State Chem 35:128
335. Zhou Z, Ye J, Arakawa H (2003) Int J Hydrogen Energy 28:663
336. Sayama K, Arakawa H (1994) J Photochem Photobiol A Chem 77:243
337. Takahara Y, Kondo JN, Takata T, Lu D, Domen K (2001) Chem Mater 13:1194
338. Kato H, Kudo A (1998) Chem Phys Lett 295:487
339. Kato H, Kudo A (1999) Catal Lett 58:153
340. Kato H, Kudo A (2001) J Phys Chem B 105:4285
341. Kato H, Asakura K, Kudo A (2003) J Am Chem Soc 125:3082
342. Yamakata A, Ishibashi T, Kato H, Kudo A, Onishi H (2003) J Phys Chem B 107:14383
343. Hur SG, Kim TW, Hwang SJ, Park H, Choi W, Kim SJ, Choy JH (2005) J Phys Chem B 109:15001
344. Hwang DW, Kim HG, Kim J, Cha KY, Kim YG, Lee JS (2000) J Catal 193:40
345. Kudo A, Kato H, Nakagawa S (2000) J Phys Chem B 104:571
346. Kato H, Kudo A (2001) J Photochem Photobiol A Chem 145:129
347. Kudo A, Nakagawa S, Kato H (1999) Chem Lett 1197
348. Kato H, Kudo A (1999) Chem Lett 1207
349. Hatanaka N, Kobayashi T, Yoneyama H, Tamura H (1982) Electrochim Acta 27:1129
350. Domen K, Kudo A, Shinozaki A, Tanaka A, Maruya K, Onishi T (1986) J Chem Soc Chem Commun 356
351. Yoshimura J, Kudo A, Tanaka A, Domen K, Maruya K, Onishi T (1988) Chem Phys Lett 147:401
352. Kudo A, Tanaka A, Domen K, Maruya K, Aika K, Onishi T (1988) J Catal 111:67
353. Kim YIl, Salim S, Hug MJ, Mallouk TE (1991) J Am Chem Soc 113:9561
354. Sayama K, Tanaka A, Domen K, Maruya K, Onishi T (1990) J Catal 124:541

355. Saupe GS, Waraksa CC, Kim HN, Han YJ, Kaschak DM, Skinner DM, Mallouk TE (2000) Chem Mater 12:1556
356. Domen K, Yoshimura J, Sekime T, Tanaka A, Onishi T (1990) Catal Lett 4:339
357. Yoshimura J, Ebina Y, Kondo J, Domen K (1993) J Phys Chem 97:1970
358. Liou YW, Wang CM (1996) J Electrochem Soc 143:1492
359. Fang M, Kim CH, Saupe GB, Kim HN, Waraksa CC, Miwa T, Fujishima A, Mallouk TE (1999) Chem Mater 11:1526
360. Takata T, Furumi Y, Shinohara K, Tanaka A, Hara M, Kondo JN, Domen K (1997) Chem Mater 9:1063
361. Kudo A, Kato H (1997) Chem Lett 867
362. Kudo A, Okutomi H, Kato H (2000) Chem Lett 1212
363. Zhou Z, Ye J, Sayama K, Arakawa H (2001) Nature 414:625
364. Miseki Y, Kato H, Kudo A (2005) Chem Lett 34:54
365. Domen K, Kudo A, Tanaka A, Onishi T (1990) Catalysis Today 8:77
366. Takata T, Tanaka A, Hara M, Kondo JN, Domen K (1998) Catalysis Today 44:17
367. Kudo A (2001) J Ceramic Soc Jpn 109:S81
368. Domen K, Hara M, Kondo JN, Takata T, Kudo A, Kobayashi H, Inoue Y (2001) Korean J Chem Eng 18:862
369. Kudo A (2003) Catalysis Surveys from Asia 7:31
370. Kato H, Kudo A (2003) Catalysis Today 78:561
371. Kudo A, Kato H, Tsuji I (2004) Chem Lett 33:1534
372. Koffyberg FP, Benko FA (1980) Appl Phys Lett 37:320
373. Lu G, Li S (1992) Int J Hydrogen Energy 17:767
374. Kudo A, Ueda K, Kato H, Mikami I (1998) Catal Lett 53:229
375. Kudo A, Hijii S (1999) Chem Lett 1103
376. Konto R, Kato H, Kobayashi H, Kudo A (2003) Phys Chem Chem Phys 5:3061
377. Yin J, Zou Z, Ye J (2003) Chem Phys Lett 378:24
378. Bessekhouad Y, Trari M, Donmerc JP (2003) Int J Hydrogen Energy 28:43
379. Saito N, Kadowaki H, Kobayashi H, Ikarashi K, Nishiyama H, Inoue Y (2004) Chem Lett 33:1452
380. Shannon RD, Rogers DB, Prewitt CT (1971) Inorg Chem 10:713
381. Rogers DB, Shannon RD, Prewitt CT, Gillson JL (1971) Inorg Chem 10:723
382. Schaak RE, Mallouk TE (2002) Chem Commun 706
383. Hwang DW, Kim HG, Lee JS, Kim J, Li W, Oh SH (2005) J Phys Chem B 109:2093
384. Aroutiounian VM, Arakelyan VM, Shahnazaryan GE (2005) Solar Energy 78:581
385. Murata Y, Fukuta S, Ishikawa S, Yokoyama S (2000) Solar Energy Mater Solar Cells 62:157
386. Baeck SH, Jaramillo TF, Brändli C, McFarland EW (2002) J Comb Chem 4:563
387. Kudo A, Mikami I (1998) Chem Lett 1027
388. Shiyanovskaya I, Hepel M (1999) J Electrochem Soc 146:243
389. de Tacconi NR, Chenthamarakshan CR, Rajeshwar K, Pauporte' T, Lincot D (2003) Electrochem Commun 5:220
390. Serpone N, Borgarelo E, Grätzel M (1984) Chem Commun 342
391. Guruswamy V, Bockris JO'M (1979) Solar Energy Materials 1:441
392. Liou FT, Yang CY, Levine SN (1982) J Electrochem Soc 129:342
393. Siripala W, Ivanovskaya A, Jaramillo TF, Baeck SH, McFarland EF (2003) Solar Energy Mater Solar Cells 77:229
394. Nozik AJ (1977) Appl Phys Lett 30:1791
395. Ohashi K, McCann J, Bockris JO'M (1977) Nature 266:610
396. Nakato Y, Takamori N, Tsubomura H (1982) Nature 295:312